



## History of late Pleistocene glaciations in the central Sayan-Tuva Upland (southern Siberia)

Sergei G. Arzhannikov<sup>a,\*</sup>, Regis Braucher<sup>b</sup>, Marc Jolivet<sup>c</sup>, Anastasia V. Arzhannikova<sup>a</sup>, Riccardo Vassallo<sup>d</sup>, Alain Chauvet<sup>e</sup>, Didier Boulès<sup>b</sup>, Frédéric Chauvet<sup>b</sup>

<sup>a</sup> Institute of the Earth's Crust, Russian Academy of Sciences, Siberian Branch, Lermontova 128, 664033 Irkutsk, Russian Federation

<sup>b</sup> CEREGE, UMR7330, CNRS, Aix Marseille Univ., BP80, 13545 Aix en Provence, France

<sup>c</sup> Géosciences Rennes, UMR6118, CNRS – Université Rennes 1, Campus de Beaulieu, 35042 Rennes Cedex, France

<sup>d</sup> LGCA, Université de Savoie, Le Bourget du Lac, France

<sup>e</sup> Laboratoire Géosciences Montpellier, CNRS-UMR5243, Université Montpellier II, Montpellier, France

### ARTICLE INFO

#### Article history:

Received 7 August 2011

Received in revised form

6 June 2012

Accepted 8 June 2012

Available online 16 July 2012

#### Keywords:

Late Pleistocene glaciations

Cosmogenic <sup>10</sup>Be

Southern Siberia

East Sayan Ridge

Moraines

### ABSTRACT

This work describes the history of late Pleistocene glaciations in the central Sayan-Tuva Upland (southern Siberia). Geological and geomorphological analysis as well as <sup>10</sup>Be surface-exposure dating revealed the glacier fluctuations in this continental area. The available published data show that the glaciers were formed in the MIS 6 and probably survived in the MIS 5. Data are also available concerning glacial advances in different periods of MIS 4, MIS 3 and MIS 2. ELAs were 2030–2230 m. Two distinct <sup>10</sup>Be exposure ages groups are highlighted reflecting the time of formation of glacial deposits in the MIS 2 associated to the Big Sayan Ridge outlet glaciers. The Sentsa – Sailag group (terminal moraine) has a mean exposure age of  $16.44 \pm 0.38$  ka. The Jombolok (terminal moraine) – Jombolok (outwash plain) group has a mean exposure age of  $22.80 \pm 0.56$  ka. The last glaciation that occurred at MIS 2 is characterized by the absence of ice cap on the Azas volcanic Plateau and of ice field in the Todza Basin. The thickness of the valley glacier was 300–400 m. At MIS 2, the terminal moraines were ~1300–1400 m a.s.l. in the Tissa, Sentsa, Jombolok and Sailag river valleys.

© 2012 Elsevier Ltd. All rights reserved.

### 1. Introduction

This work presents a synthesis of the published literature on glaciations in the eastern part of the Sayan-Tuva Upland area (Big Sayan Ridge, Todza Basin, Oka Plateau and Azas volcanic Plateau) (Fig. 1). Newly acquired in situ produced cosmogenic <sup>10</sup>Be data associated to a detailed geomorphologic study have then been used to constrain the chronology of the late Pleistocene glaciations in this region.

The analysis of Quaternary glacial deposits in southern Siberia and northern Mongolia recently provided some answers to unsolved questions on glacial sedimentation in this region (Matsera, 1993; Nemchinov et al., 1999; Krivonogov et al., 2005; Gillespie et al., 2008; Krivonogov, 2010). The ages of the glacial and lacustrine deposits were estimated and glaciations-related structures were mapped (Matsera, 1993; Yarmolyuk et al., 2001; Sugorakova et al., 2003; Komatsu et al., 2007, 2009; Gillespie et al., 2008; Krivonogov, 2010).

Many geomorphological landforms resulting from late Pleistocene glaciers activity are preserved within the Sayan-Tuva Upland and make it possible to reconstruct the paleoenvironment using various independent approaches. For example, most of the Quaternary volcanoes in the Azas volcanic province were formed in a subglacial environment (Yarmolyuk et al., 2001; Sugorakova et al., 2003; Komatsu et al., 2007). Using the size, structure, morphology and age of the tuya-volcanoes it is possible to constrain the position and thickness of the overriding glaciers. Another example is the formation of the Darhad Lake and the geomorphic evolution of the Darhad Basin (Fig. 1). The outlet glaciers extending from the Big Sayan Ridge ice field toward the south formed a glacial dam in Shishid-Gol valley. Studying and dating the various lake deposits associated to this dam allowed reconstructing the advance of glaciers in the Darhad Basin (Krivonogov et al., 2005; Gillespie et al., 2008; Komatsu et al., 2009).

Considering the role of glaciation in the evolution of the relief of the Eastern Sayan, Matsera (1993) presents the data on glacial and alluvial deposits in nine cross-sections of the Todza Basin and Azas volcanic Plateau. According to TL age estimate for burnt sub-basalt deposits (160 ka), the glacial maximum was after the emplacement

\* Corresponding author. Tel.: +7 3952 429534; fax: +7 3952 426900.  
E-mail address: sarzhan@crust.irk.ru (S.G. Arzhannikov).

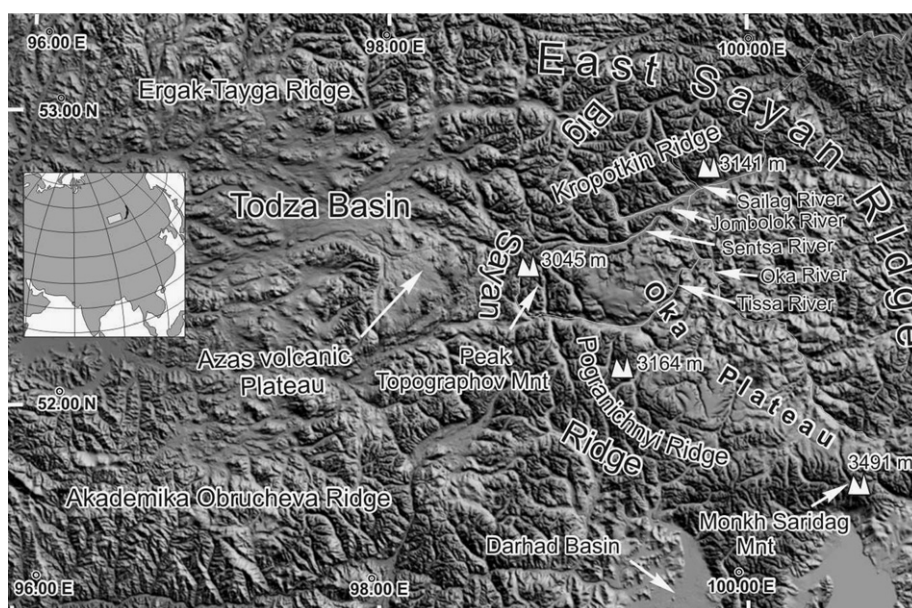


**Fig. 1.** Location map and topography of the investigated area with indications of the main orographic structures. (Topography from 90-m SRTM (Shuttle Radar Topography Mission)).

of the basaltic lava flow. No moraine deposits are found in pre-basalt sediments (Matsera, 1993).

This work intends to estimate the timing and extent of the late Pleistocene glaciations around the Big Sayan Ridge (Fig. 1). Different glacial features that developed during the various Quaternary glacial stages were dated using in situ produced cosmogenic  $^{10}\text{Be}$ . We especially focused on the marginal moraines in the Jombolok, Sentsa and Sailag river valleys. Investigations were conducted using cosmogenic isotopes geochronology ( $^{10}\text{Be}$ ), radiocarbon dating ( $^{14}\text{C}$ ), geomorphology, remote sensing data (90-m SRTM (Shuttle Radar Topography Mission)), 1:32,000 and 1:50,000 scale aerial photographs, Landsat images, 1:200,000 geological maps, 1:100,000 topographic maps, and field mapping.

## 2. Geographical setting and timing of glaciations: present knowledges

The central Sayan-Tuva Upland is a key area to understand the physical conditions and extent of glaciation in the eastern Siberian Mountains and to reconstruct the late Pleistocene paleogeography and climate of this area. In this region, the topography combines mountain ridges, elevated plateaus and deeply incised river valleys. Within the investigation area, the Todza Basin and the southern East Sayan Ridge are the major orographic structures. They include smaller-scale orographic objects such as the Big Sayan Ridge, the Oka Plateau and the Azas volcanic Plateau (Fig. 1).

The Big Sayan Ridge is located in the southern part of East Sayan Ridge, and forms the watershed between the basins of the Yenisei River and the Angara River. It consists of ridges and peaks (Fig. 1) with altitude varying between 2700 and 3491 m (the Kropotkin Ridge (3141 m), Peak Topographov (3044 m), the Pogramichnii Ridge (3164 m) and Monk-Saridag Mountain (3491 m)).

The Oka Plateau, rising up to 1800–2500 m holds a central position therein. It is characterized by a well-preserved Cretaceous – Paleogene peneplanation surface forming the main part of the plateau (Arzhannikova et al., 2011; Jolivet et al., 2011). Owing to Neogene volcanism (Rasskazov et al., 2000), part of the plateau was covered by basalt and did not undergo intensive denudation since the Miocene (Jolivet et al., 2011). The major river systems draining

the western Oka Plateau are the Jombolok, Sentsa, Tissa and Oka rivers showing measured incision depth of about 700–800 m. To the west, the Azas volcanic Plateau is covered by an accumulation of tertiary basalt sheets, Quaternary large tuya-volcanoes (with a relative height of about 500 m and an area of about 100 km<sup>2</sup>), cone-shaped volcanoes and basalt lava flows. Farther west, the Todza Basin is the largest structure of the East Tuva region and is bounded by the Akademika Obrucheva Ridge to the south and by the Ergak Tayga Ridge to the north (Fig. 1).

Since the second half of the 19th century many Pleistocene glacial features have been described in the region, providing ideas of dimensional and characteristics of Pleistocene glaciers (e.g. Kropotkin, 1867; Chersky, 1881; Voieikov, 1881; De Henning-Michaelis, 1898; Peretolchin, 1908; Molchanov, 1934).

More recently, detailed glaciological studies were conducted using remote sensing and large-scale geological survey (Obruchev, 1953; Ravskii et al., 1964; Grosswald, 1965, 1987; Olyunin, 1965) which detailed the extent of piedmont glaciations in the Todza Basin as well as mountain and valley glaciations in the East Sayan ranges. The estimated ice thickness was ranging from several hundreds of meters (East Sayan) to 1 km (Todza Basin). Glaciations were concentrated on the axial part of the Big Sayan Ridge and on the Azas volcanic Plateau. The altitude of the terminal moraines was more than 930 m in the Todza Basin and more than 740 m in the East Sayan (Grosswald, 1965; Olyunin, 1965).

New data on glacial deposits in the East Sayan Ridge and northern Mongolia ( $^{14}\text{C}$ , OSL, IRSL,  $^{10}\text{Be}$ , thermoluminescence (TL) and palynology) allowed recognition of late Pleistocene phases of glaciers extent corresponding to MIS 5d/5b, MIS 4, MIS 3 and MIS 2 (Matsera, 1993; Nemchinov et al., 1999; Krivonogov et al., 2005; Gillespie et al., 2008; Krivonogov, 2010).

The study of glacial and sub-basalt deposits in nine cross-sections of the Bii-Khem, Sorug and Azas river valleys (Fig. 2) provided important additional information on glacier dynamics for both late and middle Pleistocene (Matsera, 1993). In the Sorug valley the studies have been made into a series of cross-sections (A) and (B) (Fig. 2) whose bottom parts are composed of solid rocks, granites covered by bright-red sandy-loamy-grussy weathering crust (section A), and weathered reddish-yellow pebbles with

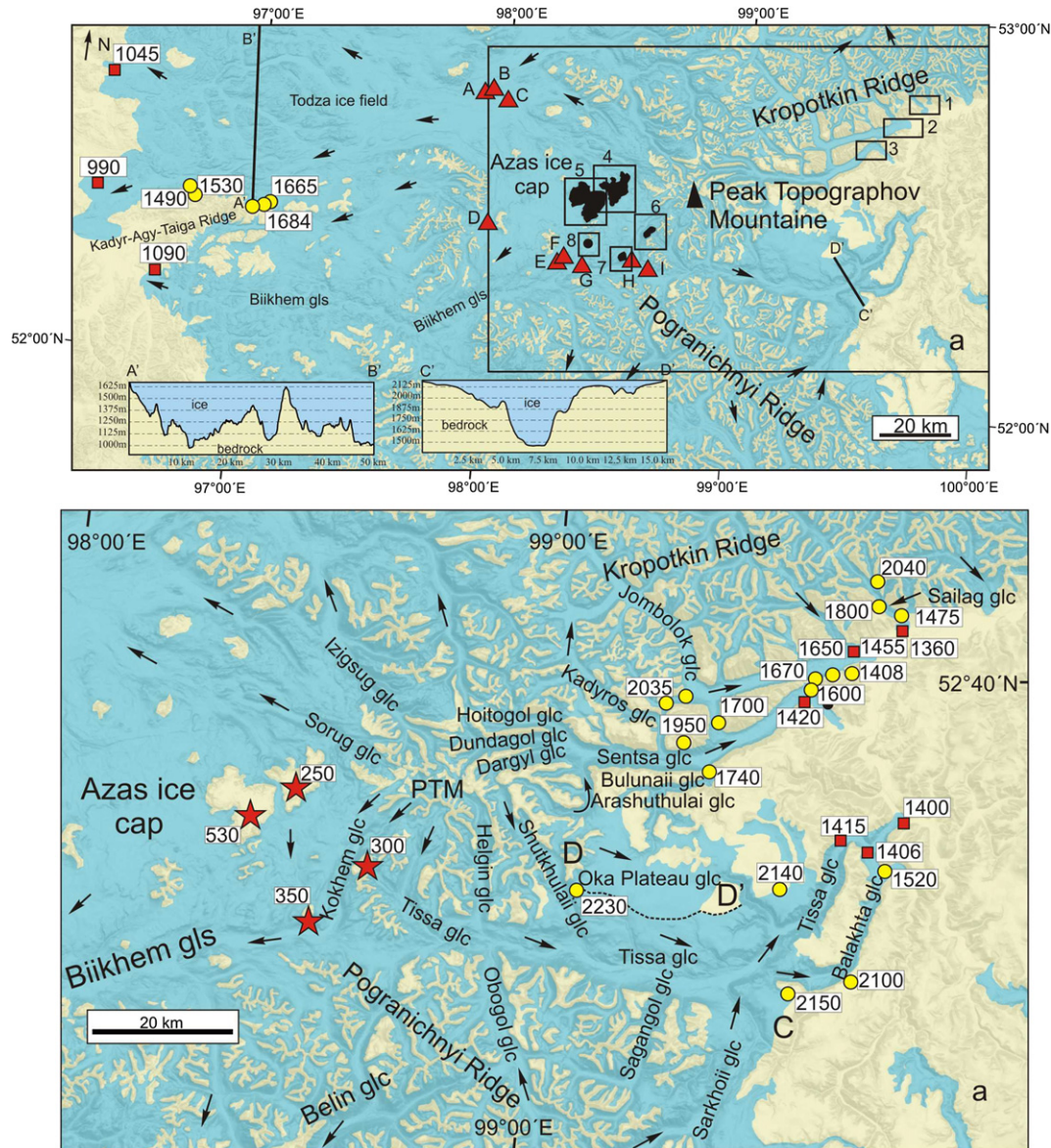


**Fig. 2.** Extent of the late Pleistocene glaciations in Todza Basin, Azas volcanic Plateau, Big Sayan Ridge and Oka Plateau (adapted from Grosswald, 1965 and Olyunin, 1965). Red stars – thickness of ice near volcano-tuya; yellow circles – altitude of the lateral moraines; red squares – max. altitude of the terminal moraines; red triangles – cross-sections (A–I) after Matsera (1993). Black line is a profile; A'B' – profile of the Todza glacier; C'D' – profile of the Tissa glacier. Black dashed line is the lateral moraine of the Tissa glacier. 1 – Sailag moraine area; 2 – Jombolok moraine area; 3 – Sentsa moraine area; 4–8 volcanoes – tuya: 4 – Sorug-Chushku-Uzu; 5 – Shivit-Taiga; 6 – Kokhemskii; 7 – Priozernyi; 8 – Ulug-Arginskii. (For interpretation of the references to color in this figure legend, the reader is referred to the web version of this article.)

sandy filler overlain by variegated clays and aleurites (section B). The weathering crust and clays in both cross-sections underlie the gray boulder-pebble deposits with ferruginized sandy-gravel filler overlain by basalt lava flowed from the Azas volcanic Plateau. The basalts are overlain by the moraine deposits. The spore and pollen analysis shows pollen spectra (section A) of pine and cedar trees admixed with those of broad-leaved trees found in the weathering crust and its overlying alluvial sediments. Cross-section (B) has exhibited a rich spectrum of broad-leaved, coniferous and deciduous plants of the Turgai flora of the Oligocene or Miocene. In the upward cross-section, thermophilic flora gives way to cold-loving plants, and there is an increase in the quantity of pollen for *Pinus silvestris*, *Pinus sibirica*, *Picea*, *Betula*, *Larix* and other species. The pollen quantity for *P. silvestris* and *P. sibirica* at the contact between basalts and alluvial sediments increases by 80–90%. The study of other cross-sections on the Azas volcanic Plateau and Todza Basin

(section A–I, Fig. 2) has shown no glacial and glacialfluvial deposits in sub-basaltic deposits. The age of basalts (160 ka) overlain by the moraine deposits has been determined by TL-dating of burnt sub-basaltic deposits (section D, Fig. 2) (Matsera, 1993). According to TL age, the glacial maximum therein began after the emplacement of the basaltic lava flow (Matsera, 1993).

Gillespie et al. (2008) showed that the late Pleistocene glaciations in the southern East Sayan Ridge appeared to be more complicated than previously inferred. For example, they concluded that the late Pleistocene glaciers around the Darhad Basin had advanced at least three times at 17–19 ka, 35–53 ka, and at an earlier, unconstrained period. The occurrence of middle Pleistocene and late Pleistocene glaciations in the southern East Sayan Ridge has also been suggested based on studies of subglacial volcanism on the Azas volcanic Plateau (Yarmolyuk et al., 2001; Komatsu et al., 2007).

The study of a section in fluvio-lacustrine deposits 100 km southeast of the Azas volcanic Plateau provided some evidences for glacial retreat in the Big Sayan Ridge. Fossil wood located 17.0–17.5 m below the surface of the sediments has been dated at  $47,500 \pm 1500$  years BP ( $^{14}\text{C}$ ) (Nemchinov et al., 1999) corresponding to MIS 3. This indicates a complete degradation of glacial ice in this part of the East Sayan Ridge. Palynological evidences attest for a considerable warming during the same period. The spore–pollen association reflects the prevalence of woody-shrub vegetation: *P. silvestris*, *P. sibirica*, *Abies*, *Picea*, *Tsuga* and others (Nemchinov et al., 1999).

High-resolution cores in Lake Kotokel (east coast of Lake Baikal) were drilled in sediments representing the last 47 ka (Bezrukova et al., 2010). The interstadial dated at 47–30 ka is characterized by cold and severe climate with the predominance of xerotic steppe and tundra steppe landscapes. During that time, there were small periods of warming as evidenced by expansion of forest-type vegetation.

Large-scale glaciation of the southeastern East Sayan at MIS 5, 4 is evidenced by red-thermoluminescence (RTL) data. The age of the Mondy moraine is  $79 \pm 9$  (RTL) and  $70 \pm 11$  (RTL) ka (Ufimtsev et al., 2003).

Data reported in Olyunin (1965) and Grosswald (1965) indicate that the late Pleistocene glacier ice thickness varied considerably in the Big Sayan Ridge, Oka Plateau, Azas volcanic Plateau and Todza Basin. This was mainly due to their location implying variable dividing-ridge orientations, size and amount of tributaries of the main glacial valleys and amount of precipitation (<http://www.geogr.msu.ru>).

## 2.1. The Kropotkin Ridge glaciation center

The Kropotkin Ridge trends SW–NE and represents the northern border of the Oka Plateau (Fig. 1). The maximum altitude of the ridge is 3149 m and it displays glacial morphological features such as U-shape valleys, glacier cirques and marginal moraines. The Kropotkin Ridge glaciers that extended toward the south were 15–20 km long, the largest outlet being the Jombolok glacier (due to their present remote and highly inaccessible position, the glaciers which extended to the north and the northeast are not considered in this paper). The Jombolok and Sailag glaciers described below are typical of the southern flank of Kropotkin Ridge and will serve as examples (Fig. 2).

### 2.1.1. Jombolok glacier features

The Jombolok glacier was located in the Jombolok valley (Fig. 2) and had a length of 63 km. The average width of the Jombolok valley is 1.5–2.5 km for a depth varying from about 100 m to 800 m. The tributaries and the ice field, located in the Kropotkin Ridge, were the source of ice for the Jombolok glacier. In the Dede-Hutal Pass (Fig. 3a), where the Jombolok glacier deposited lateral moraines, the ice was approximately 450 m thick. The lateral moraine ridges, indicative of a large glacial thickness, have been preserved upstream from the terminal moraine on the right side of the valley. In the Dodo-Hutel Pass a lateral moraine fragment is preserved at an altitude of ~1670 m (Fig. 3a). Further down in the valley, fragments of the corresponding lateral moraine (based on SRTM data) in two tributary basins are preserved at altitudes of 1670 m and 1650 m respectively (Fig. 3a). Finally, 500 m further down the valley the Jombolok glacier flowed to the adjacent valley through a low Mongoljon Pass (Fig. 3a) and left a roughly 30 m height terminal moraine.

The Jombolok marginal moraine is located 4 km the up-valley of the confluence of the Jombolok and Oka Rivers (Fig. 4). Its frontal part is located at an altitude of 1300 m and its central part has been eroded by the Jombolok River. The longitudinal profile of the

preserved fragments shows three ridges separated from each other by small depressions (Fig. 4e). The surface of the moraine is thus arranged in a series of ridges and hollows resulting from melting off of buried ice blocks. Some of those hollows became closed lakes.

### 2.1.2. Sailag glacier features

The Sailag valley is located in the Kropotkin Ridge and is a left tributary of the Oka River. During the late Pleistocene glaciation it contained a 15 km long glacier (Fig. 2). The accumulation and formation of ice occurred at an altitude of 2900–3100 m. The lateral moraine consists of a series of extended ridges or steps and has been intensively washed out by the lateral tributaries of the Sailag River. However, the main glacial valley still contains some well-preserved fragments exposed at different altitude levels. On the right side of the valley at the mouth of the Hara-Jalga River one fragment of the right lateral moraine is preserved at an altitude of 1800 m (Figs. 3b and 5b). The lowest lateral moraine is located on the right side of the Sailag valley above the mouth of the Hara-Jalga River where it has an altitude of 1725 m (Figs. 3b and 5b). It can be traced downstream to an altitude of 1460 m. The left lateral moraine shows two steps. The upper level continuous lateral moraine extends for 3.5 km from the left tributary Tsahas River (1800 m a.s.l.) down to the left tributary Ekhe-Sagin-Sair River (1575 m a.s.l.). The lower level moraine fragment is 1300 m long and is clearly visible from 1520 m to 1440 m (a.s.l.) (Fig. 5b). The central part of the marginal moraine left by the Sailag glacier has been washed out by the Sailag River, leaving only a few ridges in the Oka valley. This marginal moraine, culminating 80 m above the Oka valley floor appears as a complicated system of ridges, thermokarst basins and inter-ridges depressions.

Therefore, the study of the fragments of marginal moraines in the Sailag valley indicates at least two-phase change of the glacier parameters, probably related to different stages of glaciation. The absence of marginal moraines in the valley upwards from the Sailag marginal moraine shows a rapid glacial retreat and disappearance during the last glaciation.

## 2.2. Peak Topographov Mountain glaciation center

This area comprises a group of mountain peaks culminating around 2700–3000 m (a.s.l.) in the central part of the Big Sayan Ridge (Fig. 2). Peak Topographov Mountain was a major glaciation center in the late Pleistocene and from there, large glaciers were flowing to the West and East. The Tissa, Halgin and Shuthulaii glaciers advanced to the south into the main valley of the Tissa River and, associated to the right tributary glaciers of the Tissa River formed a c. 20 km wide large ice field (Fig. 2). The Dargil, Dunda-Gol, Hoito-Gol and Ara-Shuthulaii glaciers advanced eastward and formed the Sentsa glacier. The Kokhem glacier flowed to the south and then to the west as a part of the large Biihem glacier. Finally the Sorug and Izigsug glaciers were part of the major Todza glacier. The present glaciers with marginal moraines are located in the northern and eastern cirques of Peak Topographov Mountain.

### 2.2.1. Glaciation features on the Oka Plateau

The Oka Plateau is an upland with altitudes of 1800–2500 m. According to the geological and geomorphological mapping, glacial and glaci-fluvial deposits are widely distributed on the surface of the Oka Plateau (Geological map, N-47-XXXIV, 1971). Moraine deposits are mainly preserved at the bottom of the eastern slope of Peak Topographov Mountain, to the north and east from Pogranichnyi Ridge (Fig. 2). On the relief they represent 50–100 m high hills.

These sediments were deposited by glaciers moving down the eastern spurs of the Peak Topographov Mountain toward the Oka Plateau. At the piedmont, these glaciers merged and formed the

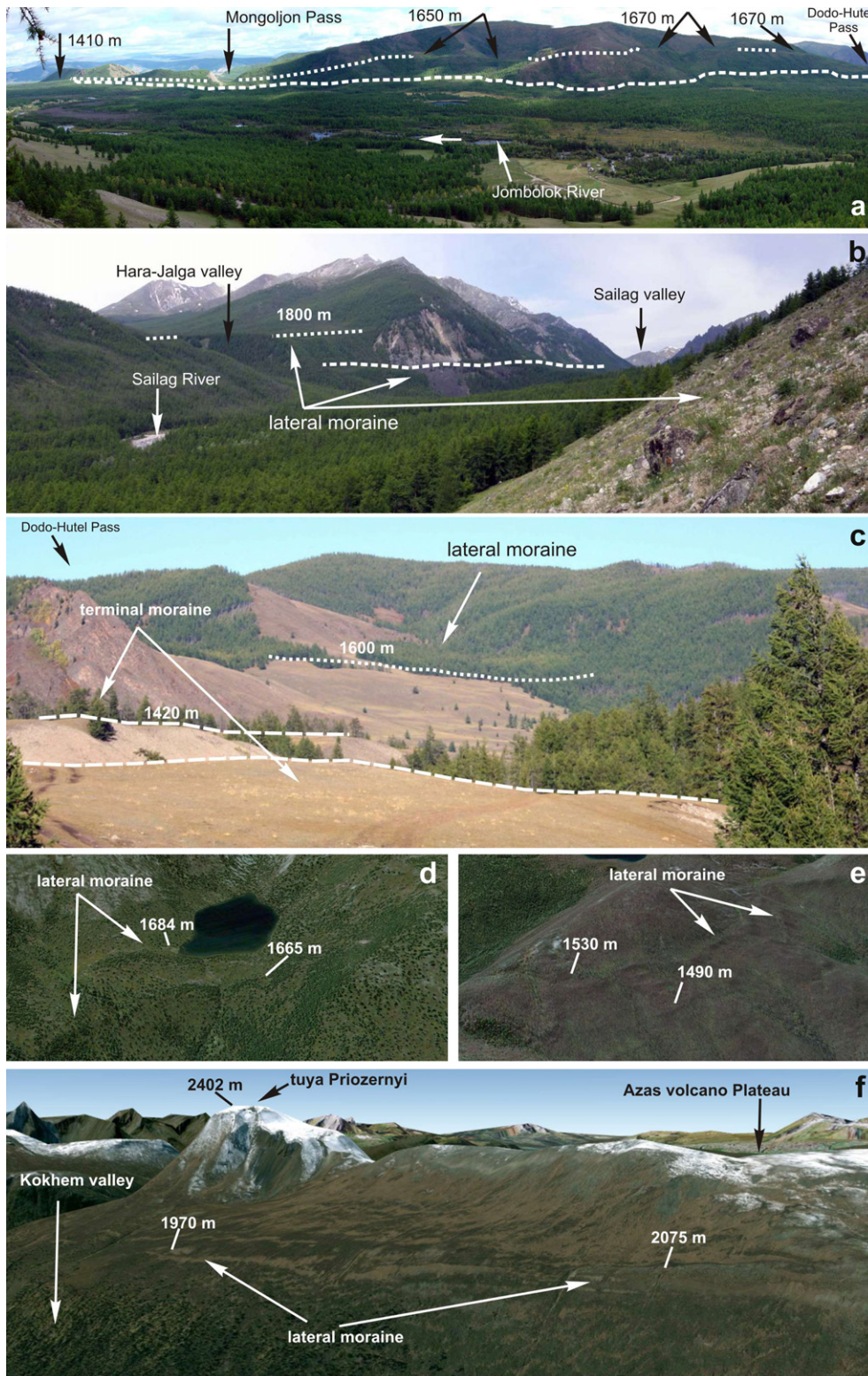


**Fig. 3.** Photographs (a, b, c) and 3d (d, e, f) model SRTM data and GeoEye satellite images (Google Earth) showing location and altitude of the lateral moraines. a – Jombolok valley; b – Sailag valley; c – Sentsa valley; d, e – Todza Basin; e – right side of Kokhem valley and tuya Priozernyi.

Oka Plateau glacier. The glacier moved predominantly southeastward. In the southeast, the Oka Plateau glacier joined with the largest Tissa valley glaciers of the East Sayan Ridge, forming a large glacial field (Fig. 2). In the north, some parts of the Oka Plateau

glacier connected with the Sentsa glacier through the outlet glacier. To the east of the Peak Topographov Mountain, on the surface of the Oka Plateau there are some granite massifs that fed small glaciers in the late Pleistocene (Fig. 2).

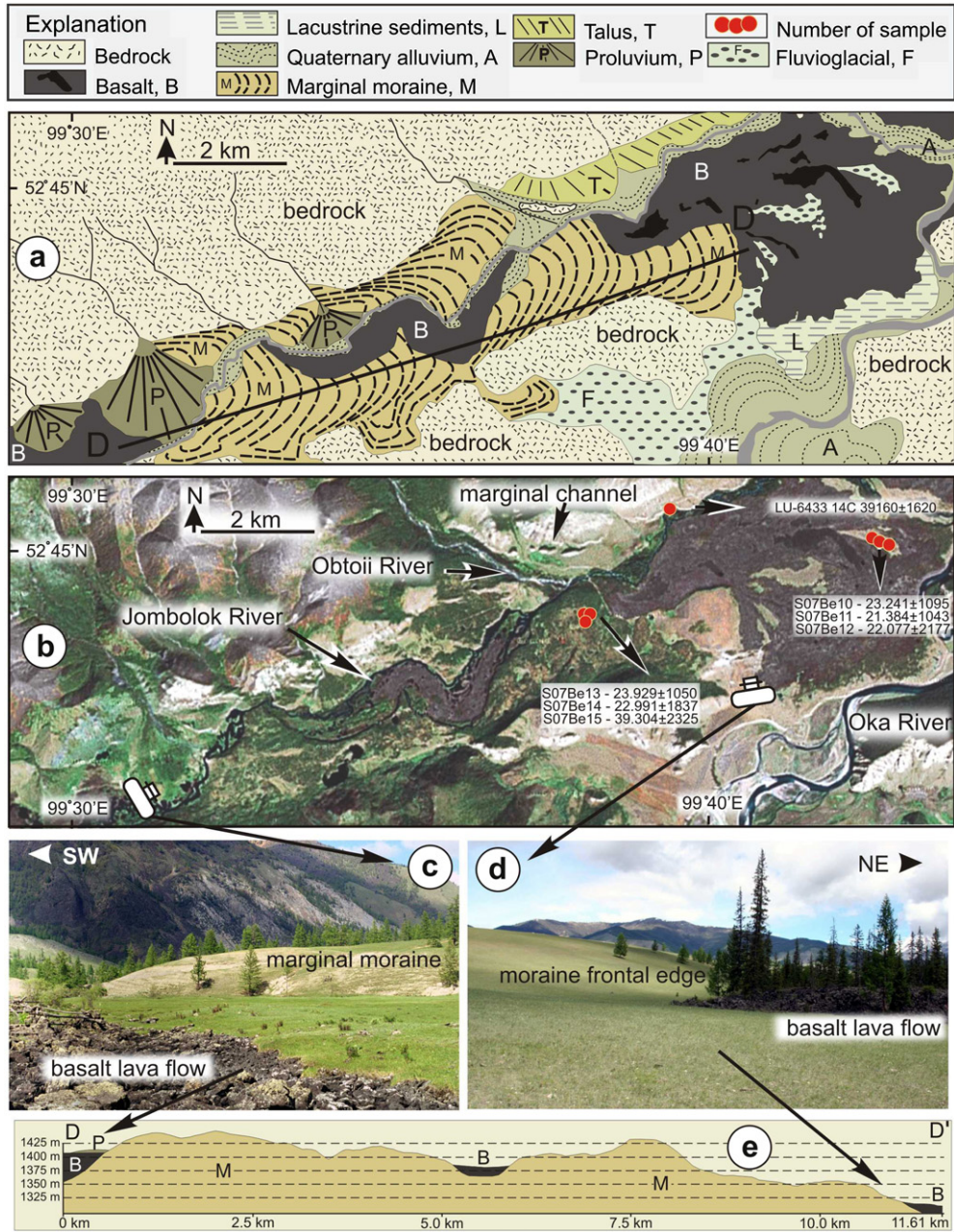


**Fig. 4.** Jombolok terminal moraine and basalt lava flow located in the Oka and Jombolok river valleys. (a) Schematic drawing of the Quaternary deposits (b) Fragment of the Landsat satellite image with references to sampling sites and <sup>10</sup>Be and <sup>14</sup>C ages. (c) A scarp on the backside of the terminal moraine. (d) Frontal part of the terminal moraine. (e) Longitudinal profile DD' of the Jombolok terminal moraine.

2.2.2. Features of the Tissa glacier

The Tissa glacier was located within the Peak Topographov Mountain and flowed to the east over a distance of 105 km before reaching the Oka River. The glacier was formed by large iceflows issued from the Peak Topographov Mountain (left tributaries: Helgin, Shuthulaii glaciers) and the Pogranichniy Ridge (right tributaries: Obogol, Sagangol and Sarkhoii glaciers) (Fig. 2). At altitudes of 2200 m the ice was advancing toward the edge of the Oka Plateau and joined with the local ice field. North of the Tissa valley on the surface of the Oka Plateau preserved fragments of the left lateral moraine indicate an ice thickness of about 700 m for the Tissa glacier (Fig. 2, profile CD). The Tissa glacier was flowing over a low pass to the Balakhta valley after its confluence with the Sarkhoii glacier (Fig. 2). There it formed two “tongues” that were

merging again after 50 km. Complex lateral moraines, marginal channels and kames terraces are exposed on the most favorable slopes of the Tissa valley. In some cases, the glacial deposits completely cover the valley slope from 2200 m to 1500 m. In the Tissa valley, two end moraines are preserved: a 50 m high terminal moraine is located at the mouth of the Tissa River. Three kilometers upstream a second terminal moraine is preserved.

2.2.3. The Sentsa glacier features

This 55 km long, glacier was located north of the Tissa glacier, in the Sentsa valley (Fig. 2). The Sentsa glacier was formed by the junction of three large glaciers (Hoito-Gol, Dunda-Gol and Dargyl), associated to tributaries coming down from the Kropotkin Ridge and the Oka Plateau (Ara-Shuthulaii and Bulunaii glaciers). In the

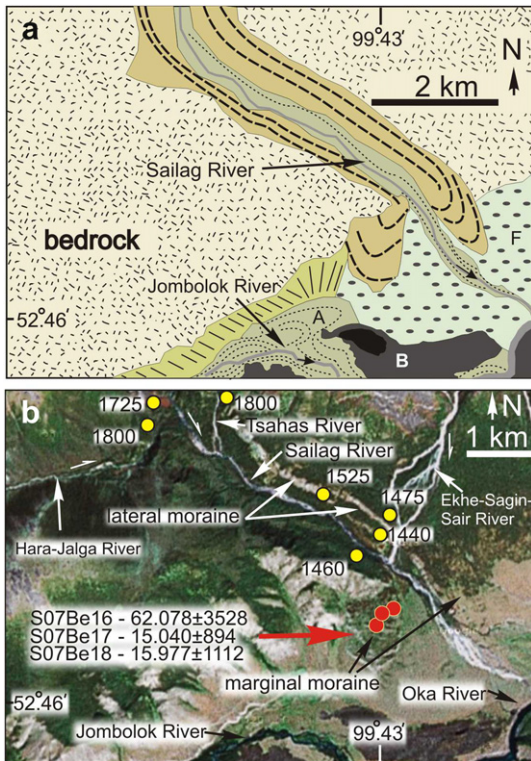


**Fig. 5.** Sailag marginal moraines. (a) Schematic drawing of Quaternary deposits. (b) Fragment of the Landsat satellite image with references to sampling sites and  $^{10}\text{Be}$  ages. The yellow circles indicate the altitudes of the lateral moraines. (For interpretation of the references to color in this figure legend, the reader is referred to the web version of this article.)

left tributary, located 2 km downstream from the mouth of the Kadyr-Os River a fragment of lateral moraine sits at an altitude of 1950 m (Fig. 2). In the Bulunaii valley another fragment is preserved at an altitude of 1740 m and a third one is preserved at 1700 m in the Dede-Hutel Pass (Fig. 2). Glacial deposits are also present on the left bank of the Sentsa River at an altitude of 1600 m (Fig. 3c). It should be noted that in the Sentsa valley a lower level of lateral moraines is preserved at altitudes of 1450–1500 m. The Sentsa glacier ended about 8.5 km upstream of the Sentsa river mouth where it left a thick marginal moraine about 8 km in length. In this segment, glacial deposits completely filled the Sentsa valley (Fig. 6) with a thickness of 90 m. The surface of the terminal moraine is a complex of various ridges, hills and rounded or elongated depressions. The topography of the terminal moraine shows fragments of 22–45 m high ridges (above the mean surface of the moraine) oblique to the valley. The minimum and maximum altitude of the Sentsa terminal moraine are respectively 1380 m and 1470 m.

#### 2.2.4. Outwash plains of the Jombolok and Sentsa moraines

Outwash plains are widespread in the river valleys of the Oka Plateau. They are formed by accumulation of glacial material transported by melt-water. A system of braided streams develops within which coarse-grained material is transported and deposited. A longitudinal slope ( $5^\circ$ ) characterizes the outwash plains located in front of the Sentsa terminal moraine. A complex system of braided streams that varies in width from 1.8 to 2.5 km developed on the surface of the outwash plain. A similar relief, partly buried by young basaltic lava flows, is observed in the outer part of the terminal moraine in the Jombolok river valley (Fig. 4a,b). The upper surface of the outwash plain is typically isolated between erosion

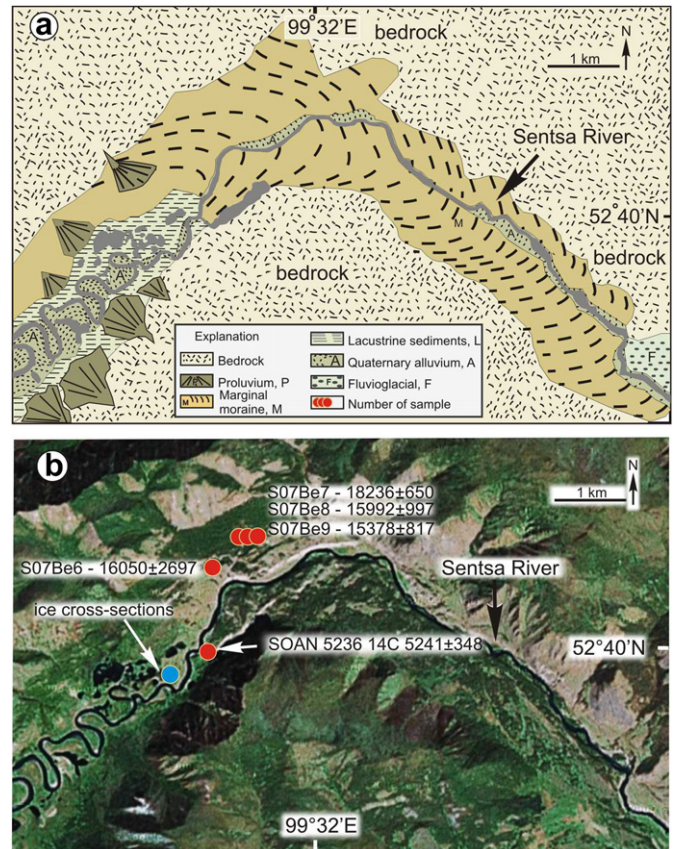


**Fig. 6.** Sentsa terminal moraine. (a) Schematic drawing of the Quaternary deposits. (b) Fragment of the Landsat satellite image with references to sampling sites and  $^{10}\text{Be}$  and  $^{14}\text{C}$  ages. Blue circle is the buried ice discovered in the Sentsa River valley. (For interpretation of the references to color in this figure legend, the reader is referred to the web version of this article.)

channels and the resulting difference in elevation prevented some fragments of the surface from being buried by basaltic lava flows. Those fragments are now represented by isolated “windows” of glacial deposits (Fig. 7).

#### 2.2.5. The Kokhem glacier

This glacier was located in the Kokhem valley and corresponded to the upper reaches of the major, 170 km long Bii-khem glacier (Fig. 2). The existence of this glacier is indicated by the Kokhemskii and Priozernyi volcano-tuyas that formed in a subglacial environment. Based on the height of the volcanoes located on both sides of the Kok-Khem valley, the ice thickness reaches 500 m on the Azas volcanic Plateau and 750 m in the Kok-Khem valley. On the right and left slopes of the Kok-Khem valley several lateral moraines are exposed below the base of the volcanoes corresponding to an estimated ice thickness of 300–350 m (Fig. 3e). Progressive downstepping of the lateral moraines in the Kok-Khem, Tissa and Sentsa valleys illustrates the reduction of ice thickness through time.

### 2.3. The Azas volcanic Plateau glaciation center

The 2000 m high Azas volcanic Plateau belongs to the East Tuva volcanic province and covers an area of more than 2000 km<sup>2</sup>. Most of the large volcanoes located on the Azas volcanic Plateau were formed in subglacial environment during the Pleistocene (Table 1). Earlier volcanoclastic series on the Azas volcanic Plateau were described as volcanic tuffs (Grosswald et al., 1959), however

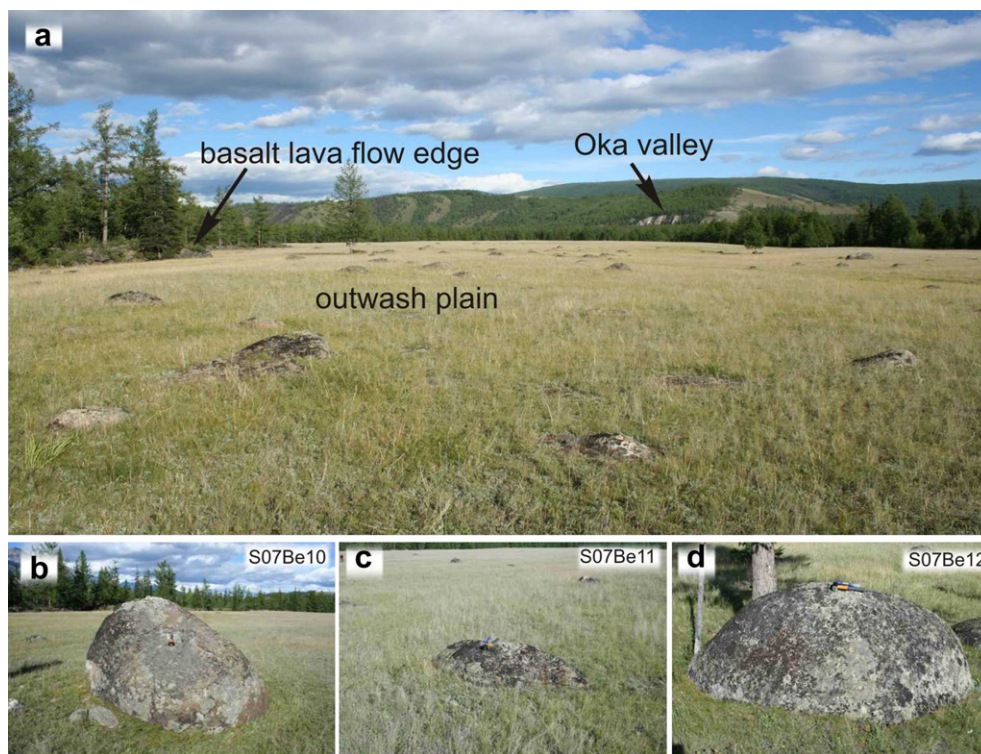


**Fig. 7.** Top: photograph showing a fragment of the outwash plain surface preserved in the frontal part of the Jombolok terminal moraine. The three bottom photographs present the dated boulders.

volcanic edifices were later identified as subglacial volcanoes (Grosswald, 1965; Yarmolyuk et al., 2001; Sugorakova et al., 2003).

Similar general features are observed on all the Azas volcanoes: they are located on the plateau and appear like 400–600 m high table mountains (Fig. 8a–d). Their surface is flat or dome-shaped with abrupt, sometimes strong eroded slopes. Each volcanic edifice is formed by a basal volcanoclastic layer (70% or more of the total volume) capped by a lava layer. Ash cones are located on the surface of most of the volcanoes (Sugorakova et al., 2003).

K/Ar dating of subglacial volcanoes has been performed at IGEM RAS, Novosibirsk (Yarmolyuk et al., 2001) using isotope dilution technique with  $^{38}\text{Ar}$  tracer (Table 1). Analytical details can be found in Yarmolyuk et al. (2001). Calculations of radiogenic  $^{40}\text{Ar}$  were done assuming that initial (background) argon isotope composition is equal to atmospheric ( $^{40}\text{Ar}/^{36}\text{Ar} \equiv 295.5$ ). The age errors associated to the K/Ar method are sometimes larger than the duration of the inter-glacial stages and those data thus have to be used carefully. Komatsu et al. (2007) noted that the morphologically older volcanoes were effectively associated to the older K/Ar ages. To provide reliable indications on the age of the various late Pleistocene glaciation periods, the K/Ar ages must thus be used in conjunction with the geomorphological description of the dated volcanoes.

The 2648 m high (SRTM data) tuya Kokhemskii (Figs. 8a and 9) is located on the left side of the Kok-Khem River valley. The thickness of the hyaloclastite layer is 300 m and a K/Ar age of  $150 \pm 50$  ka was obtained by Yarmolyuk et al. (2001). About 300 m of ice covered the Azas volcanic Plateau during the formation of the Kokhemskii volcano, similar to the one around the Sorug-Chushku-Uzu volcano. Once again the western slope of the volcano shows traces of glacial erosion.

Shivit-Taiga (Figs. 8b and 9) is one of the largest subglacial volcanoes in the Azas volcanic Plateau. It has a surface area of about

100 km<sup>2</sup> and a height of 500 m. Yarmolyuk et al. (2001) reported an age of  $110 \pm 40$  ka and  $130 \pm 40$  ka (K/Ar).

The western slopes of the Shivit-Taiga volcano were glaciated at least once after the retreat of the Azas ice cap. Two terminal moraines are clearly visible on aerial photographs at the toes of the Shivit-Taiga (Fig. 10). The maximal altitude of the top level of the hyaloclastite is 2725 m (SRTM data), implying that the thickness of the ice in this area some 110 to 130 ka ago was not less than 530 m (Fig. 9).

The 2525 m high (SRTM data) Sorug-Chushku-Uzu tuya (Figs. 8d and 9) is located 1 km northeast of the Shivit-Taiga volcano. The thickness of the hyaloclastite layer is 200–250 m (Fig. 9) and the K/Ar age obtained for the volcano is  $60 \pm 40$  ka (Yarmolyuk et al., 2001). The thickness of the ice contemporaneously to the eruption of the Sorug-Chushku-Uzu was 200–250 m. The slopes of the volcano are deformed by landslides and in some places the western slope of the volcano was eroded by a glacier which formed a U-shaped valley and cirques.

The 2401 m high Priozernyi volcano is located on the right side of the Kok-Khem valley. Its base is formed by a 300–350 m thick layer of hyaloclastite with a K/Ar age of  $75 \pm 40$  ka (Yarmolyuk et al., 2001).

The Ulug-Arginskii volcano is located in a glacial cirque 5 km south of the Shivit-Taiga volcano. It formed after a phase of glacial erosion which removed the volcanic series deposited on the piedmont of the Shivit-Taiga volcano during previous eruptions. The Ulug-Arginskii volcano consists of ash and lava flows and is dated (K/Ar) at  $48 \pm 20$  ka (Yarmolyuk et al., 2001). It is a cone-shaped structure with a diameter of 800 m, a height of 150 m and a summit altitude of 2263 m (SRTM data). The formation of the volcano occurred in surficial environment after the retreat of the glacier on the Azas volcanic Plateau.

Morphological and age analysis of the valley basalts in the Bii-Khem River also constrain the ice retreat in this valley. No K/Ar



**Table 1**  
Types and ages of volcanic units in the study area (from Yarmolyuk et al., 2001).

$N^{\circ}$ of samples (name of volcanoes)	Main types of volcanics	Main mode of eruption	K, % ( $\pm\sigma$ )	$^{40}\text{Ar}_{\text{rad}}$ , ng/g ( $\pm\sigma$ )	Age, ka ( $\pm 1.6\sigma$ )
UA – 1/5 (Ulug-Arginskii vlc.)	Hyaloclastite	Subglacial	$1.68 \pm 0.03$	$0.0056 \pm 0.0006$	$48 \pm 20$
Sch – 1/4 (Sorug-Chushku-Uzu vlc.)	Hyaloclastite	Subglacial	$1.82 \pm 0.02$	$0.0075 \pm 0.0025$	$60 \pm 40$
Pr – 1/7 (Priozernyi vlc.)	Hyaloclastite	Subglacial	$1.54 \pm 0.02$	$0.0081 \pm 0.0025$	$75 \pm 40$
Sht – 1/1 (Shivit-Taiga vlc.)	Hyaloclastite	Subglacial	$1.40 \pm 0.03$	$0.0104 \pm 0.0021$	$110 \pm 40$
Sht – 1/8 (Shivit-Taiga vlc.)	Hyaloclastite	Subglacial	$1.14 \pm 0.03$	$0.0098 \pm 0.0015$	$130 \pm 40$
Pr – 3/3 (Kokhemskii vlc.)	Hyaloclastite	Subglacial	$1.82 \pm 0.02$	$0.019 \pm 0.004$	$150 \pm 50$

age is available for these basalts but as they cover a basanit flow from the Ulug-Arginskii volcano they are thus younger than the  $48 \pm 20$  ka age obtained for this last volcano. The valley basalts have flown along the Bii-Khem River valley on some tens of kilometers

and in some places lay in the river. Their thickness exceeds 50 m and they cover older glacial deposits within which some basaltic dykes have been intruded (Sugorakova et al., 2003).

#### 2.4. Pogranichnii Ridge glaciation center

This is the largest and highest orographic structure of the Big Sayan Ridge (Figs. 1 and 2), with a length of 155 km and many mountain crests higher than 3000 m. Mount Monk-Saridag, located at the eastern end of the Pogranichnii Ridge has a maximum altitude of 3491 m. In the Pogranichnii Ridge glaciers (Obogol, Hohurjalga, Horingol, Sagangol and Sarkhoi glaciers) were flowing toward the north-north-east and connected with the Tissa glacier. To the south-west the Tengisgol and Belin glaciers were two major ice tongues.

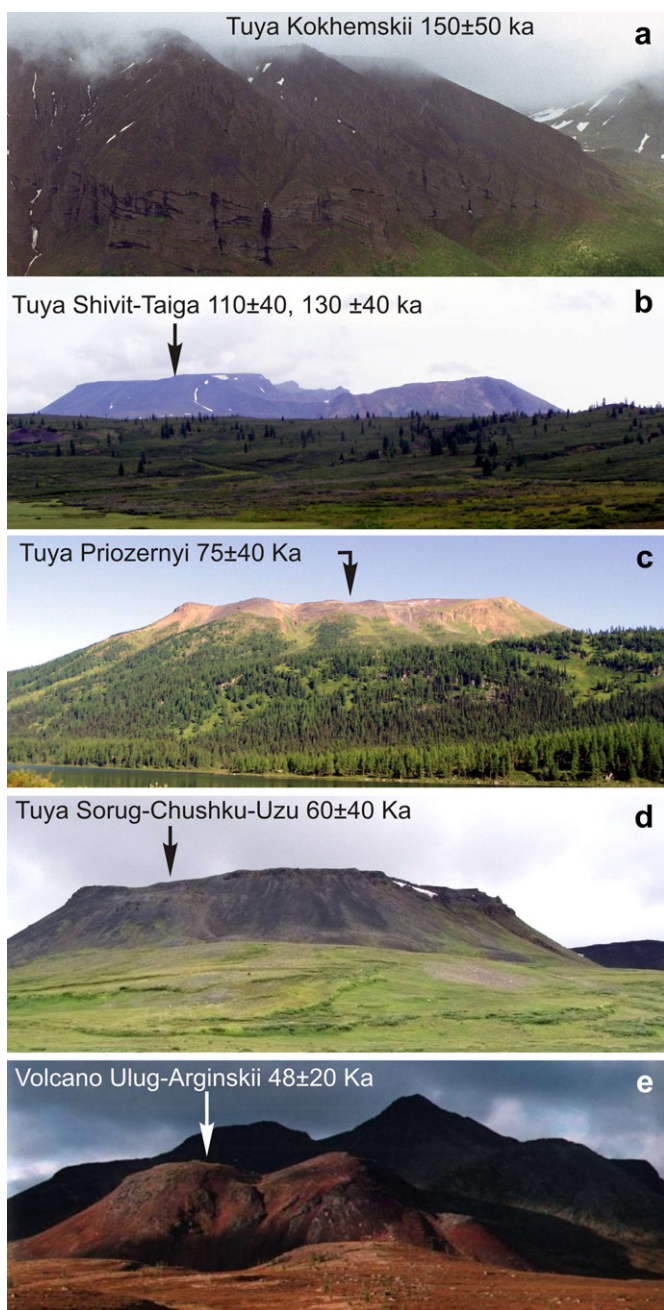


**Fig. 8.** Field photographs showing the volcanoes formed on the Azas volcanic Plateau. (a, b, c, d) volcanoes erupted through ice cap. (e) Ulug-Arginskii volcano formed in the aerial environment.

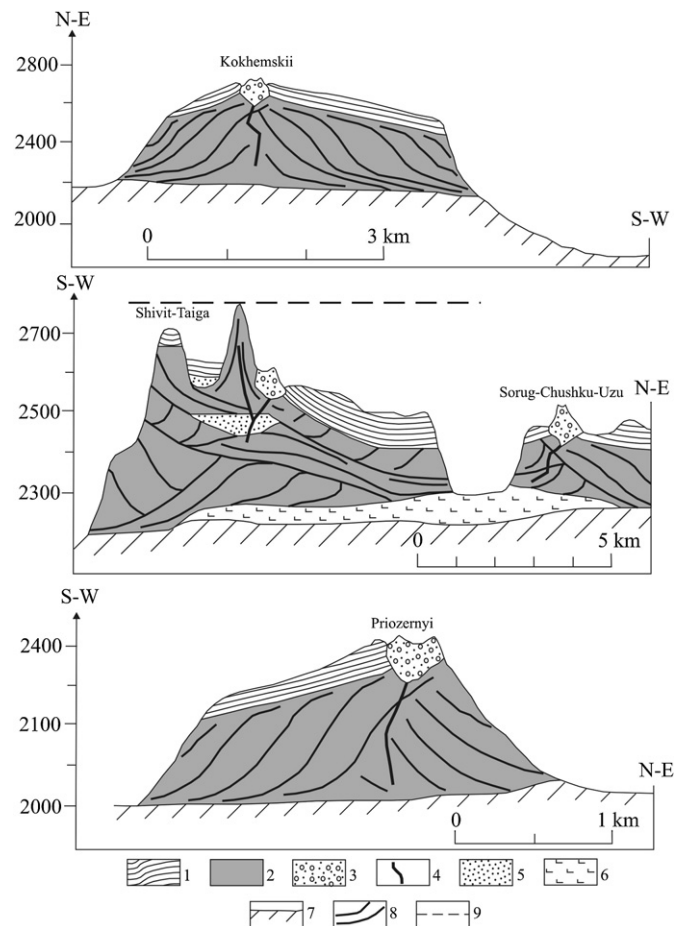


**Fig. 9.** Structure of volcanic edifices. Based on Sugorakova et al., 2003. 1–4 – Volcanic deposits: 1 – Lava flows, 2 – Volcaniclastic series, 3 – Ash cones, 4 – Feeding dykes; 5 – Lacustrine deposits (sandstones, gravelstones, siltstones); 6 – Lava plateau series; 7 – Bedrock; 8 – Limits of volcaniclastic stratiform units; 9 – Suggested upper limit of ice.

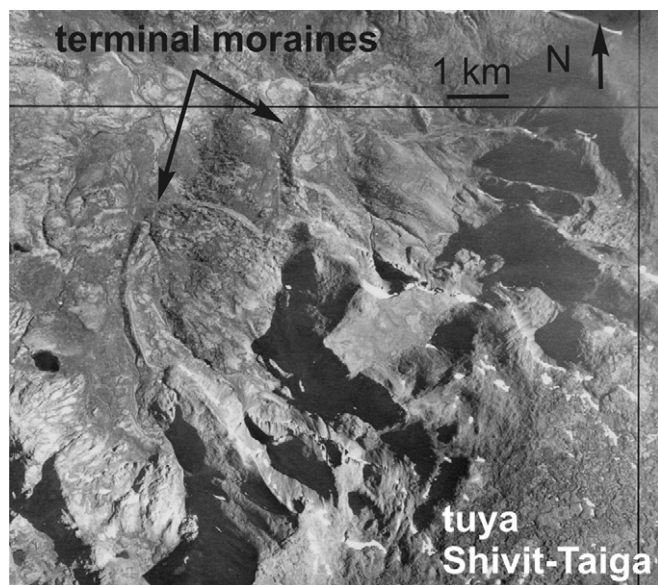


Fig. 10. Terminal moraines on the piedmont of the Shivit-Taiga tuya. Aerial photographs.

### 3. Reconstruction of equilibrium line altitudes (ELA)

The palaeo ELAs have been estimated using the data obtained in the reconstruction of glaciers in the Sailag, Jombolok, Sentsa and Tissa river valleys (Tables 2 and 3). For the Big Sayan Ridge the ELA during the late Pleistocene glaciations was determined from Median Elevation of Glaciers (MEG) (Meierding, 1982), Toe-to-Headwall Altitude Ratio (THAR) and Maximum Elevation of Lateral Moraines (MELM) (Andrews, 1975; Nesje and Dahl, 2000). THAR is the ratio between the toe of the glacier and the top of the valley headwall (Leonard and Fountain, 2003). The THAR method provides a simple and relatively rapid way of assessing palaeo-ELA. However it requires defining the headwall limit of the studied glacier. Based on SRTM data THAR palaeo-ELAs were calculated in this study using ratios of 0.5 (e.g. Benn and Lehmkuhl, 2000; Gillespie et al., 2008). The MEG is the median elevation of a glacier (Meierding, 1982). MELM method is based on the idea that the uppermost altitude of an abandoned lateral moraine marks the palaeo-ELA. Here the height of lateral moraines was estimated using the SRTM data, Landsat satellite images and aerial photographs (1949–1964 years). The highest lateral moraine was taken as the ELA. According to these data the late Pleistocene ELAs in the Big Sayan Ridge were most probably between 2030 m a.s.l. and 2230 m a.s.l.

### 4. $^{10}\text{Be}$ surface exposure dating

Minimum ages of glacial deposits were obtained from measurements of in situ produced  $^{10}\text{Be}$  concentrations in quartz from granite and granodiorite boulders exposed within moraines

Table 2  
Parameters of the palaeoglaciers.

Glacier	Area (km <sup>2</sup> )	Main tongue length (km)	Morphology	Min a.s.l.	Max a.s.l.
Tissa	1345	105	Valley glacier	1400	3045
Sentsa	474	60	Valley glacier	1420	2720
Jombolok	648	66	Valley glacier	1455	2640
Sailag	66	18	Valley glacier	1360	2730

Table 3

The reconstruction ELAs of the late Pleistocene glaciers in the Big Sayan Ridge.

Glacier	Reconstructed equilibrium line altitude (m a.s.l.)			
	Thar (0.5)	Meg	Melm	Mean
Tissa	2222	2222	2240	2228
Sentsa	2070	2070	1950	2030
Jombolok	2048	2048	2035	2043
Sailag	2045	2045	2040	2043

and outwash plains. Samples were taken from the top of boulders belonging to three terminal moraines or, in one place, to the surface of the outwash plain. The geographic position and altitude of the samples were obtained using a portable GPS (uncertainty  $\pm 5$  m). For each sample, the topographic shielding and surface inclination were measured (Table 4). To select the most suitable sampling sites on the moraines, different parameters were taken into account: subhorizontal surfaces, maximum distance from the slopes (to prevent solifluction) and absence of thermokarsts depressions.

In total, 13 samples were collected. 10 samples belong to the outlet glaciers of the Peak Topographov Mountain ice field and three samples to the outlet glacier of the Kropotkin Ridge ice field. Four samples (S07Be6, S07Be7, S07Be8 and S07Be9) were taken from the terminal moraine in the Sentsa valley (Fig. 6b). Three samples were taken from boulders on the middle-ridge surface (S07Be13, S07Be14, S07Be15) in the Jombolok River valley (Fig. 4b) 10 km north-east from the Sentsa's samples. The terminal moraine area in the sampling site is characterized by a flat, partially forested surface with a slight degree of curvature. Three samples (S07Be10, S07Be11 and S07Be12) were taken from large boulders on the outwash plain 2.5 km from the Jombolok terminal moraine (Fig. 7). The surface of the outwash plain at the sampling site is a "window" free from basaltic lava. We assume that within those isolated windows, the boulders have been protected from flowing water and thus from significant erosion. Finally, three samples were collected in different parts of the Sailag terminal moraine (Fig. 5b). Sample S07Be16 was taken from the crest of the moraine and samples S07Be17 and S07Be18 were taken from the inner part of the terminal moraine.

Quartz-rich samples were prepared for cosmogenic nuclide concentration measurements following chemical procedures adapted from Brown et al. (1991) and Merchel and Hergers (1999). After addition in each sample of  $\sim 100$   $\mu\text{l}$  of an in-house  $3.10\text{--}3$  g/g  $^9\text{Be}$  carrier solution prepared from deep-mined phenakite,  $^{10}\text{Be}$  and  $^{26}\text{Al}$  measurements were performed at the French AMS National Facility, ASTER, located at CEREGE in Aix-en-Provence.  $^{10}\text{Be}$  data were calibrated directly against the National Institute of Standards and Technology standard reference material 4325 by using an assigned values of  $(2.79 \pm 0.03) \times 10^{-11}$  and a  $^{10}\text{Be}$  half-life of  $(1.387 \pm 0.012) \times 10^6$  (Chmeleff et al., 2010; Korschinek et al., 2010). Analytical uncertainties (reported as  $1\sigma$ ) include uncertainties associated with AMS counting statistics, AMS external error (0.5%), chemical blank measurement. Long term measurements of chemically processed blank yield ratios on the order of  $(3.0 \pm 1.5) \times 10^{-15}$  for  $^{10}\text{Be}$  (Arnold et al., 2010).

Stone (2000) polynomial has been used to determine surficial production rate assuming a SLHL production rate of  $4.49$  at  $\text{g}^{-1} \text{a}^{-1}$  for  $^{10}\text{Be}$ . The obtained surface production rates were then only corrected for local slope and thickness since topographic shielding due to surrounding morphologies was insignificant for all samples. In order to determine exposure ages from the  $^{10}\text{Be}$  concentrations measured in the quartz fractions, the following equation was used:

**Table 4**  
Description of samples dated by  $^{10}\text{Be}$  cosmogenic nuclides.

Sample	Localization	Diameter (m)	Latitude	Longitude	Altitude	Topographic shielding	Stone scaling	$^{10}\text{B}$ at/g	Exposure age (y)
S07BE6	Sentsa valley terminal moraine	0.5	52°.6804	99°.50675	1443	0.998	3.58	253,722 ± 42,628	16,050 ± 2697
S07BE7		0.4	52°.68243	99°.509	1445	0.999	3.58	288,783 ± 10,291	18,236 ± 650
S07BE8		0.4	52°.68246	99°.50875	1453	0.999	3.61	254,954 ± 15,901	15,992 ± 997
S07BE9	Jombolok terminal moraine front	0.4	52°.68273	99°.50905	1453	0.999	3.61	245,138 ± 13,024	15,373 ± 817
S07BE10		2.0	52°.75221	99°.70855	1293	0.999	3.18	326,675 ± 15,396	23,241 ± 1095
S07BE11		1.2	52°.75213	99°.70725	1294	0.999	3.18	300,936 ± 14,674	21,384 ± 1043
S07BE12		1.4	52°.7525	99°.70508	1294	0.999	3.18	310,635 ± 30,629	22,077 ± 2177
S07BE13		0.8	52°.74003	99°.63303	1420	0.999	3.52	371,290 ± 16,293	23,929 ± 1050
S07BE14	Jombolok valley terminal moraine	0.8	52°.7398	99°.633183	1420	0.999	3.52	356,826 ± 28,508	22,991 ± 1837
S07BE15		0.4	52°.7397	99°.63337	1413	0.999	3.50	604,157 ± 35,732	39,304 ± 2325
S07BE16		1.2	52°.777116	99°.718416	1383	0.998	3.42	925,983 ± 52,619	62,078 ± 3528
S07BE17	Sailag valley terminal moraine	0.9	52°.777683	99°.718616	1385	0.998	3.42	227,390 ± 13,519	15,040 ± 894
S07BE18		0.8	52°.778333	99°.721216	1385	0.999	3.42	241,671 ± 16,821	15,977 ± 1112

Samples have a density of 2.5 and are ~3 cm thick. Samples were crushed, sieved (0.5–1 mm) and chemically etched. Pure quartz was dissolved in HF in the presence of  $^9\text{Be}$  carrier (100 µg of  $3.025 \times 10^{-3}$  g/g  $^9\text{Be}$  solution). Ion exchange columns (Dowex 1x8 and 50Wx8) were used to extract  $^{10}\text{Be}$ .  $^{10}\text{Be}/^9\text{Be}$  ratios were measured by accelerator mass spectrometry at ASTER the French National Facility (CEREGE, Aix-en-Provence). Concentrations are reported relative to NIST SRM4325 standard, using an assigned value for the  $^{10}\text{Be}/^9\text{Be}$  ratio of  $2.79 \times 10^{-11}$  and a  $^{10}\text{Be}$  half-life of 1.387 Ma (Korschinek et al., 2010). A sea level high latitude spallation production rate of  $4.49 \pm 0.29$  atoms  $\text{g}^{-1} \text{y}^{-1}$  and the stone scaling factors (Stone, 2000) were applied. Muons scheme is based on Braucher et al. (2003).

$$C_{(x,\varepsilon,t)} = \frac{P_{\text{spall.}}}{\Lambda_n + \lambda} \cdot e^{-\frac{x}{\Lambda_n}} \left[ 1 - \exp\left\{ -t \left( \frac{\varepsilon}{\Lambda_n} + \lambda \right) \right\} \right] + \frac{P_{\mu_{\text{slow}}}}{\Lambda_{\mu_{\text{slow}}} + \lambda} \cdot e^{-\frac{x}{\Lambda_{\mu_{\text{slow}}}}} \left[ 1 - \exp\left\{ -t \left( \frac{\varepsilon}{\Lambda_{\mu_{\text{slow}}}} + \lambda \right) \right\} \right] + \frac{P_{\mu_{\text{fast}}}}{\Lambda_{\mu_{\text{fast}}} + \lambda} \cdot e^{-\frac{x}{\Lambda_{\mu_{\text{fast}}}}} \left[ 1 - \exp\left\{ -t \left( \frac{\varepsilon}{\Lambda_{\mu_{\text{fast}}}} + \lambda \right) \right\} \right]$$

where  $C_{(x,\varepsilon,t)}$  is the  $^{10}\text{Be}$  concentration as a function of depth  $x$  ( $\text{g}/\text{cm}^2$ ),  $\varepsilon$ , the denudation rate ( $\text{g}/\text{cm}^2/\text{yr}$ ) and  $t$  the exposure time (yr);  $P_{\mu_{\text{slow}}}$  and  $P_{\mu_{\text{fast}}}$  are the contributions due to slow and fast muons (Braucher et al., 2003).  $\Lambda_n$ ,  $\Lambda_{\mu_{\text{slow}}}$ , and  $\Lambda_{\mu_{\text{fast}}}$  are the effective apparent attenuation lengths ( $\text{g}/\text{cm}^2$ ), for neutrons, slow muons, and fast muons, respectively. All calculations were performed using attenuation lengths of 160, 1500, and 5300  $\text{g}/\text{cm}^2$  (Braucher et al., 2003). Exposures ages do not take into account geomagnetic field and solar output changes through time since no agreement arise yet in the community; however all data are provided (Table 5) to perform such correction through the CRONUS-Earth online calculator (<http://hess.ess.washington.edu/>; Balco et al., 2008).

**Table 5**  
Cosmogenic  $^{10}\text{Be}$  weighted mean exposure ages.

	Age (a)	Theoretical 95% Chi-square	Experimental 95% Chi square	Theoretical 95% Chi-square	Experimental 95% Chi square	Weighted mean age (analytical uncertainties)
Sentsa + Sailag group	S07BE6	16,050 ± 2697	12.59 (n = 7)	11.07 (n = 6)	11.05	16,443 ± 376
	S07BE7	18,236 ± 650				
	S07BE8	15,992 ± 997				
	S07BE9	15,373 ± 817				
	S07BE17	15,040 ± 894				
	S07BE18	15,977 ± 1112				
	S07BE16	62,078 ± 3528				
Jombolok group	S07BE10	23,241 ± 1095	11.07 (n = 6)	9.49 (n = 5)	3.28	22,798 ± 561
	S07BE11	21,384 ± 1043				
	S07BE12	22,077 ± 2177				
	S07BE13	23,929 ± 1050				
	S07BE14	22,991 ± 1837				
	S07BE15	39,304 ± 2325				

Outliers have been discarded using a Chi-square test. Regarding the numbers of samples ( $n$ ) per moraines, the 0.05 critical value for a Chi-square with  $(n - 1)$  degrees of freedom is calculated (Experimental value) and compared with the theoretical one given by Chi-square table. If the calculated value is lower than the theoretical one, then all samples are used to calculate a weighted mean exposure age; if not, outliers are rejected, until the distribution passes the test and the weighted mean exposure age is calculated with the remaining samples.

#### 4.1. Factors controlling the quality of the data

One of the main conditions for obtaining quality data is the physical stability through time of the dated boulders. Ideally, the analyzed boulder should be stabilized during the retreat of the glacier and its orientation in space must be fixed at that time. However, following the retreat of the glacier, the boulders are exposed to other physical processes that affect their stabilization on the surface of the moraine. These include: erosion (bottom and lateral erosion of the river draining the moraine), solifluction and thermokarst. In order to study the influence of the above mentioned processes in our sampling sites we examined the morphology of cross sections within the terminal and lateral moraines, the terraces, and the outwash plains. We especially focus on evidences of cryogenic deformations that reflect the dynamics of movement in the seasonally thawed layer. To get an information on the post-deposition behavior of the sediments, deposits varying from clay sediments to coarsely fragmented rocks were investigated. The following conclusions have been drawn for each phenomena:

- Downcutting and lateral erosion of watercourses can significantly deform the surface of a moraine. However, water erosion

is localized in a narrow sector and only destroys parts of the moraine. In this case areas of elevated moraines (especially on terminal moraines) such as their crests, are preserved, showing stable subhorizontal surfaces.

- Solifluction is a plastic-viscous flow of wetted fine sediments moving down the slopes. To initiate solifluction it is necessary to get abundant silt deposits, water and surface slopes from 2–3° to 10–15° free of trees and bushes. Solifluction is widespread, actively developing in mountainous and lowland tundra but rarely in the taiga. The slope exposure appears to play a significant role in the development of solifluction. Solifluction in the Baikal area is located on the northern slopes. At the same time on the dry slopes of southern exposure solifluction does not develop (Romanovskii, 1993).

The Jombolok cross section (Fig. 11a) is located at the base of the southern slope of the Kropotkin Ridge. The 10 m thick section consists of layers of sand, gravel, boulders, unsorted not rounded fragments of rocks and buried soil horizons. The lower soil horizon has an age of  $39,160 \pm 1620$  BP (Fig. 11a) (Arzhannikov et al., 2010). By observing and studying the different depths of sediments we saw no significant cryogenic deformation in the form of cryoturbation and solifluction structures of the flow. In our opinion the absence of cryogenic deformation is determined by the southern exposure slope and the occurrence of permeable sediments in most of this section.

The Sentsa cross section I is located on the left bank of the Sentsa River (Fig. 11b). The 3 m deep cross section of sandy sediments and buried soil has been studied within the floodplain. The lower part of the frozen sand deposits with no visible cryogenic deformation is found at a depth of 2.5 m.

The 1 m deep Sentsa cross section II (Fig. 11c) is located on the right bank of the Sentsa River (Fig. 6b) near the upstream slope of the terminal moraine. Glacial deposits strongly affected by landfire and dated at  $5248 \pm 348$  BP (SOAN Lab, Novosibirsk, Russia) are located at the base of the profile (Fig. 11c). Above them are white silt and peat. No indications of solifluction or cryoturbation could be found in this profile.

The Oka cross section (Fig. 11d,e) is located 2 km south-east of the Jombolok terminal moraine on the left bank of the Oka River. The cross section is composed of lacustrine-fluvial deposits that were formed in basalt flow dammed lake in the Oka River valley. The profile is about 5 m deep and is composed of alluvial sands leaning against the basalt flows (Fig. 11d). Because of this geometrical relation the age of the sand deposits cannot exceed the age of the 7000 BP basalts that blocked the Oka river (Ivanov et al., 2011). Small cracks with a displacement of 1 cm are observed in the profile probably due to post-depositional gravitational movements on the river banks and small ice wedges. However, no large-scale cryogenic deformation could be observed.

#### 4.1.1. Thermokarst

Development of thermokarst involves thawing ice sediment and ground ice. When the ice melts, the surface subsides creating various forms of meso- and microrelief. The distribution, morphology and depth of the thermokarst lakes are determined by the cryogenic structure of the deposits (the presence and size of ice derived from various sources) (Romanovskii, 1993). The existence of dry and water-filled depressions on the surface of the moraine reveals the formation of thermokarst during the retreat and melting of the glacier. In the Sentsa valley, ice remains at a depth of 1 m below the ground surface (Fig. 11g). Potential modern reactivation of thermokarst processes in the valley is indicated by changes in the shoreline of various lakes and immersion of trees that initially grew on the lake shores (Fig. 11f) (Arzhannikov et al.,

2010). However, the present processes are restricted to the Sentsa River valley and do not affect the lateral moraines or terminal moraines complex. Well-preserved large subhorizontal surfaces on top of the moraines indicate the absence of any active thermokarst processes within those moraines over a long period of time, possibly since the retreat of the glacier.

Based on the above description of the various profiles, the following conclusions can be drawn: 1) Permafrost and buried ice occur in the study area; 2) Large cryogenic deformation and solifluction in the sections younger than 40,000 years were not found; 3) Thermokarst formation processes are still active in areas where buried ice is preserved, but they do not affect the marginal moraines; 4) The bottom and lateral erosion of the river draining the moraine.

Another important factor of physical stability through time of the dated boulders is the original form of a marginal moraine.

Putkonen and O'Neal (2006) showed that the moraine having steep slope angles and sharp crest undergoes an intensive denudation after glacial retreat which provides smoothing of the original glacial relief and significant rejuvenation for exposure ages. This is true for single marginal ridges though there are also some other forms of a marginal moraine that have a more complex shape and an extensive moraine surface such as multiple crested moraines and multi-crested push moraines (Bennett, 2001). The study of the marginal moraines in the Tissa, Sentsa, Jombolok and Sailag river valleys indicated that most of them do not have classic parallel arch-like recessional and terminal ridges. Terminal and recessional moraines in the Sentsa and Jombolok river valleys are chaotic agglomerations of glacial deposits occupying the entire valley width that is 8–10 km. The concentration of terminal moraine deposits may be related to the fact that the glacier end occasionally reached this area and formed the terminal moraine within this 8–10 km during the late Pleistocene.

The fragments of marginal moraines (Sentsa, Jombolok) and outwash plain wherefrom the samples were taken usually have an angle of their surface of no more than 1–3° and an extension of 500–600 m. The relative height variation within this area is no more than 2–3 m. The Sailag valley shows somewhat different morphology that involves several ridges with short crests wherein the samples were taken.

In an effort to control the exposure ages we have used the paragenetic relationship between the moraine formation and formation of the outwash plain in the Jombolok valley. The samples taken from the marginal moraine and the outwash plain surface, in locations free from basaltic flow, are expected to show a similar age, and if they really do, we may strongly assert that glacial and water-glacial relief forms in this valley have the same age of formation.

## 5. Results

Minimum exposure ages derived from  $^{10}\text{Be}$  measurements are presented in Table 4. They show that, for each moraine, surficial concentrations are similar among boulders. Only two samples (SO7BE15 and SO7BE16 middle-ridge surface in the Jombolok River and crest of the Sailag terminal moraine, respectively) have significantly different values (these two blocks are older than the rest of their respective groups). As recently reviewed by Balco (2011) the scatter in exposure ages can be due to different processes (partial burial by soil, denudation, weathering, post depositional movement ...) and the strategies for identifying and discarding outliers are multiples. In our case, since the two considered boulders (SO7BE15 and SO7BE16) are much older than their respective neighbors, they have been considered to be previously exposed and thus the excess of  $^{10}\text{Be}$  has been considered to be inheritance. A more rigorous way to decipher if these two



**Fig. 11.** Photographs (a, b, c, d, e, f, g) showing the fragments of the cross-sections. A - Left side of Jombolok valley; b - Left bank of the Sentsa River; c - Right bank of the Sentsa River; dI,dII - Left side of Oka valley; e, f - Left bank of Sentsa River.

samples are outliers or not, is to use a statistical procedure. Thus, to combine and compare the different moraine exposure ages, the method proposed by Ward and Wilson (1978) was applied. This method is based on Chi square analysis. To obtain the most adequate number of samples ( $n$ ) per moraines, 0.05 critical value for a Chi-square with ( $n - 1$ ) degrees of freedom is calculated and compared with theoretical value given by a Chi-square table. If the calculated value is lower than the theoretical one, then all samples are used to calculate a weighted mean exposure age. Otherwise outliers are rejected until the distribution passes the test and the weighted mean exposure age is calculated with the remaining samples (Table 5). Note that as all samples have roughly the same analytical uncertainty, this statistical approach tests in fact the degree of geological scattering.

The mean weighted age for the Sentsa and Sailag group is  $16.44 \pm 0.38$  ka (6 samples). One sample (S07Be10), probably affected by isotope inheritance from previous exposure was rejected as an outlier based on a Chi-square test. The mean weighted age for the Jombolok group is  $22.80 \pm 0.56$  ka (5 samples). Again based on a Chi-square test, one sample (S07Be15) was considered as an outlier because of a cosmogenic inheritance and rejected. According to the calculated mean ages, all these moraines formed during Marine Isotope Stages MIS 2 (11–24 ka).

The samples (S07Be15 and S07Be16) have older exposure ages. A long-term exposure may be due to both previous glaciation stages and exposure in situ and, subsequently, to gravity transfer from the slope to the glacier and to glacier transfer to the place of deposition.

Sample S07Be15 has been taken from the middle-ridge surface of the Jombolok multiple moraine. Its exposure age is  $39,304 \pm 2335$  that corresponds to the period of existence of Paleolake Darkhad (53–35 ka) and advance of the Tengisgol glacier (Gillespie et al., 2008) and to the time ( $39,160 \pm 1620$ ) of soil horizon formation in the Jombolok valley (Fig. 11a) lower the Jombolok marginal moraine. Considering that the Big Sayan Ridge is a single glacial point for the Tengisgol and Jombolok glaciers, this exposure age will most likely be correlated with one of the phases of glacier advance.

The boulder wherefrom sample S07Be15 has been taken is located on the surface of one of the Sailag marginal moraine ridges. Its exposure age is  $62,078 \pm 3528$  that corresponds to the time interval of MIS 4. In this case, it is more difficult to determine cause for this older exposure age. There is a very high probability that this boulder was re-deposited. On one hand, there could be a displacement of this boulder exposed previously on the slope in situ and deposited subsequently within the marginal moraine. On the other hand, this boulder may have been deposited in earlier phases of glacier advance comparable with the glaciation phases during which some tuyas were formed on the Azas volcanic Plateau.

## 6. Discussion on the history of late Pleistocene glaciations

The Late Pleistocene glaciations within the central Sayan-Tuva Upland area were non-uniform. Most of the ice was concentrated in the Big Sayan Ridge, the Azas volcanic Plateau and the Todza Basin. Smaller glaciers developed on the Oka Plateau and in the river valleys (Fig. 2). This palaeo-distribution of the ice correlates to the modern distribution of precipitations (<http://www.geogr.msu.ru>).

Within the studied area, the present-day climate is extremely continental with negative mean annual temperatures. The mid-annual amount of precipitations is not uniform over the region and the maximal value coincides with area of high altitudes within the Big Sayan Ridge. Due to the general eastward wind direction, precipitations occur preferentially on the western slopes. Similarly the amount of precipitation in the Todza Basin and on the Oka

Plateau is 3–4 times lower than in the Big Sayan Ridge. A similar precipitation pattern can be expected for the area during the late Pleistocene.

At ELA 2030 m, the solid precipitation accumulates on a large area. This area included Big Sayan Ridge, the part of Oka Plateau and most of Azas volcanic Plateau, which gave way to the formation of large ice fields and ice caps that extended into basins and along river valleys. One of them is the Todza ice field. It initiated through the merging of glaciers on the western slope of Big Sayan Ridge. Grosswald (1965) also shared the opinion that the formation of the Todza ice field is due to the extension of glaciers from the western slope of the Big Sayan Ridge. The area of the Todza ice field was convex in shape, thickening (1300 m max) about 50 km from the glacier's margin (Grosswald, 1965).

Our studies have shown that the lateral moraines found on the slopes of the Kadyr-Agy-Taiga Ridge (Figs. 2 and 3dII) located in the Todza Basin may indicate the existence of nunataks during the late Pleistocene glaciation period. The study of lateral moraines on the range slopes in the internal ice field of the Todza Basin has shown that the glacial maximum ice was no more than 700-m thick (Fig. 2, profile AB). In the river valleys, the glacial maximum ice was as thick as 700–800 m (Bii-Khem River, Tissa River).

During the late Pleistocene glacial maximum, the glacier occupied 24,600 km<sup>2</sup> of the investigated area with an ice thickness of 500–700 m, and the ice had a volume of 12–17 thousand km<sup>3</sup>. Its formation occurred later than 160 ka (Matsera, 1993), probably in MIS 6 (Gillespie et al., 2008) coeval with global cooling (Fig. 13). This period is associated with the intensification of volcanic activity on the Azas volcanic Plateau (Yarmolyuk et al., 2001) and the formation of the Kokhemsii and Shivit-Taiga volcanoes (Table 1, Fig. 13). The Azas ice cap was more than 530 m thick when the volcano erupted. By that time, the Azas ice cap probably merged with the Peak Topographov Mountain ice field. At the same time, the glaciers moving to the west from the Big Sayan Ridge and the Azas ice cap were also merged and formed the large Todza Basin ice field. We do not have exposure ages of glacial deposits for MIS 5, though this period might have been associated with subglacial eruptions of the Shivit-Taiga and Priozernyi volcanoes (Table 1, Fig. 13). When the Priozernyi volcano erupted, the thickness of the ice on the Azas volcanic Plateau had decreased down to 300–350 m. The existence of a large ice field on the Big Sayan Ridge at the end of MIS 5 is indicated by the RTL data (Ufimtsev et al., 2003) (Fig. 13). Probable occurrence of glaciation in the Big Sayan Ridge in MIS 5d/5b was also reported by Krivonogov et al. (2005). This conclusion was based on evidences of mountain glaciation in Pribaikalye (Krivonogov et al., 2005; Krivonogov, 2010).

At MIS 4 an ice cap was overlying the Azas volcanic Plateau and, perhaps, the Todza Basin. When the Sorug-Chushku-Uzu volcano formed the still retreating ice was only 200–250 m thick.

There was a significant decrease in glacial ice thickness in river valleys of the Big Sayan Ridge and the Oka Plateau. It is likely that partial retreat of the glaciers in some massifs inside the Big Sayan Ridge occurred during the short-term warming stages. For example, it occurred in the upper reaches of the Khore River on the northern slope of the Munku-Sardyk massif (Nemchinov et al., 1999) and on the Azas volcanic plateau (Yarmolyuk et al., 2001; Sugorakova et al., 2003) (Fig. 13). During eruption of the Ulug-Arginskii volcano the ice on the plateau retreated back to the Peak Topographov Mountain, but remained in the Kok-Khem River valley. Reduction of the Todza Basin ice field resulted from the retreat of the Azas ice cap. However, the decrease of the ice cap in the Todza Basin was probably non-uniform, the Bii-khem glacier to the south being one of the first ones to melt. Full retreat of the ice in the Bii-Khem valley occurred between the formation of the Sorug-

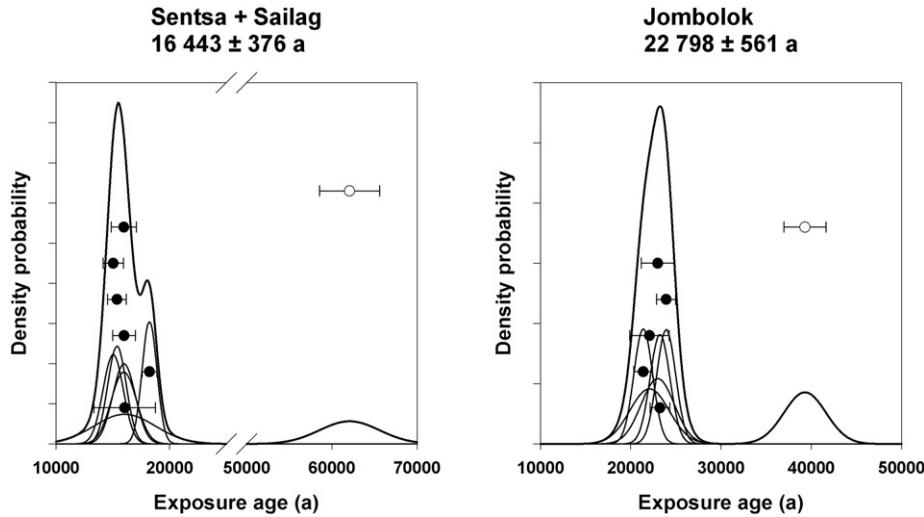


Fig. 12. Cosmogenic <sup>10</sup>Be weighted mean exposure ages.

Chushku-Uzu volcano and the emplacement of the valley basalts in the Bii-Khem River.

According to the results reported in Nemchinov et al. (1999), Krivonogov et al. (2005) and Krivonogov (2010), the glaciation at MIS 2 was restricted and did not reach the extent of the previous glaciation. The data reported by Gillespie et al. (2008) for the Darhad Basin suggest that the glaciers at MIS 2 advanced to the positions of those at MIS 3 (Fig. 13), even though their volume was smaller than that of the earlier glaciers. The data from Lake Kotokel borehole show that the last glaciation in Pribaikalye took place between 30 and 17 ka (Fig. 13) and was characterized by an increase in aridity and the development of a predominantly opened grassy landscape (Bezrukova et al., 2010).

We have studied four moraines in the valleys of the Tissa, Sentsa, Jombolok and Sailag rivers. A total of 13 <sup>10</sup>Be samples were taken from three moraines and in one place from an outwash plain. Some of these samples have been combined because the Big Sayan Ridge was a general source of ice for the investigated glaciers. Terminal moraines had no well expressed ridges.

The results are separated in two age groups which reflect the time of formation of the glacial deposits of the Big Sayan Ridge outlet glaciers. The Sentsa (terminal moraine)-Sailag (terminal moraine) group has a mean age of  $16.44 \pm 0.38$  <sup>10</sup>Be ka while the Jombolok (terminal moraine)-Jombolok (outwash plain) group has a mean age of  $22.80 \pm 0.56$  <sup>10</sup>Be ka (Figs. 12 and 13).

The exposure ages obtained from these moraine samples correlate with the last glaciation (MIS 2).

The absence of glacial deposits down the valley from the investigated moraines indicates that the glacial extent in MIS 2 reached the area of maximum distribution of sediments deposited during previous glaciations.

The age of the glacial deposits or that of the geological objects that formed simultaneously with glaciation (volcano-tuya) does not define precisely the intervals of existence for glacial ice at MIS5 and MIS 4 and is not continuously traced during these stages. The most critical point is K/Ar dates that contain a significant error and may cover large time limits. This applies especially to the young volcanoes. As to the ages of the glacial formations reported in

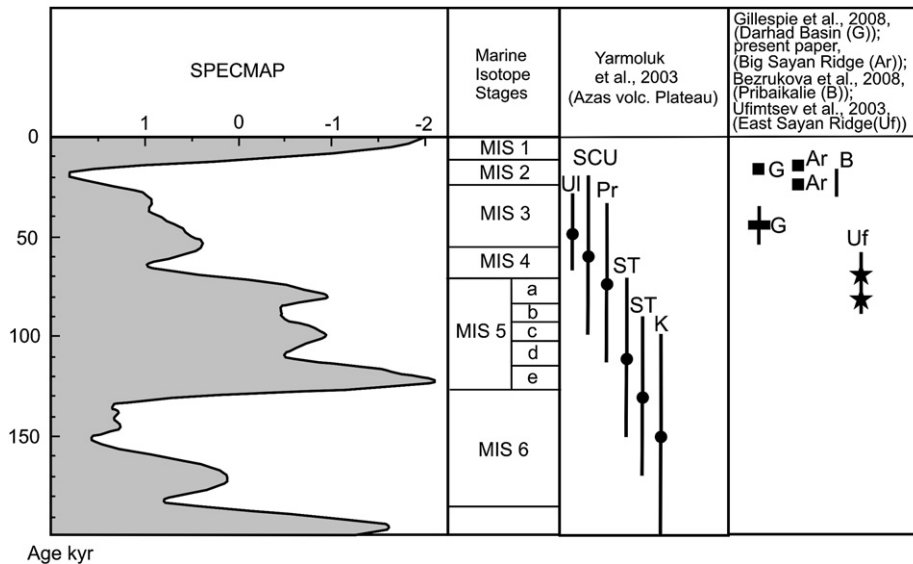


Fig. 13. K/Ar dates for subglacial volcanoes (black circles), exposure ages of Darhad Basin and Big Sayan Ridge (black squares), <sup>14</sup>C, IRSL, OSL dates of Darhad Basin – black rectangle, pollen and AMS dates of Pribaikalie (black line) and RTL dates of East Sayan Ridge (black stars). Ul – Ulug-Arginskii; SCU – Sorug-Chushku-Uzu; Pr – Priezernyi; ST – Shivit-Taiga; K – Kokhemskii.

Bezrukova et al. (2010), Gillespie et al. (2008) and present paper, there is almost continuous presence of data on glaciation in the investigated area between 53 and 16 thousand years ago.

The glaciers may have existed continuously during most of the late Pleistocene, varying gradually in size. Similar conclusions were reached by Olyunin (1965) who studied the glaciers on the eastern slope of Big Sayan Ridge, and by Matsera (1993) from the results of sedimentological investigations on the western slope of Big Sayan Ridge. However, this is only hypothetical according to the data currently available. A more complete solution to this problem needs further advanced study for the age of sub-glacial volcanoes of the Azas volcanic Plateau.

## 7. Conclusion

The Todza Basin, the Big Sayan Ridge, some parts of the Oka Plateau and the Azas volcanic Plateau as well as river valleys to the south of the East Sayan region were covered by a thick ice field. In the eastern Todza Basin, the ice was about 700 m thick while on the Azas plateau it was about 300–600 m thick, and reached about 700–800 m in the valleys of the southern East Sayan.

ELAs were comprised between 2030 m a.s.l. and 2230 m a.s.l.

The large ice field was probably formed before stage MIS 5, on the Todza Basin, the Azas volcanic Plateau and the Big Sayan Ridge. Ice buildup occurred simultaneously with the formation of the volcanoes - tuya located on the Azas volcanic Plateau. MIS 5 and MIS 4 probably do not correspond to periods of full retreat of the glaciers but rather to stages of insignificant reduction of the area and thickness of ice. This is reflected in the morphology and structure of the hyaloclastite made Priozernyi and Sorug-Chushku-Uzu volcanoes which were formed at this time in subglacial conditions (thickness of ice ~200–300 m). Significant reduction of glaciers presumably occurred on the Azas volcanic Plateau at the time of eruption of the Ulug-Arginskii volcano (MIS 3).

Cosmogenic  $^{10}\text{Be}$  was used to determine the exposure age of the boulders on different parts of the moraines and outwash plains. A mean age of  $16,443 \pm 376$  yrs was obtained for the Sentsa-Sailag moraines and a mean age of  $22,798 \pm 561$  yrs was obtained for the Jombolok moraine and outwash plain. A distinct feature of the glaciation at MIS 2 was the absence of ice cap on the Azas volcanic Plateau and in the Todza Basin. The thickness of the valley glacier decreased from 700–800 m (MIS 5, 4) to 300–400 m (MIS 2).

## Acknowledgments

This work was financed by the Russian Fund for Basic Research number 05-05-66812, 12-05-98029, the BES Russian Academy of Sciences Fund number 4.11 and by the French-Russian Programme International de Coopération Scientifique – Russian Fund for Basic Research project number 4881–09-05-91052. M. Arnold, G. Aumaître and K. Keddadouche are thanked for their valuable assistance during  $^{10}\text{Be}$  and  $^{26}\text{Al}$  measurements at the ASTER AMS national facility (CEREGE, Aix en Provence) which is supported by the INSU/CNRS, the French Ministry of Research and Higher Education, IRD and CEA. We are grateful to Jakob Heyman, Alan Gillespie and Marie-Luce Chevalier for helpful comments to improve the initial manuscript and Alexey Ivanov for scientific consultation.

## References

Andrews, J.T., 1975. *Glacial Systems: an Approach to Glaciers and Their Environments*. Duxbury Press, North Scituate, Massachusetts, 191 pp.

Arnold, M., Merchel, S., Bourles, D.L., Braucher, R., Benedetti, L., Finkel, R.C., Aumaître, G., Gott dang, A., Klein, M., 2010. The French accelerator mass

spectrometry facility ASTER: improved performance and developments. *Nuclear Instruments and Methods in Physics Research B* 268, 1954–1959.

Arzhannikov, S.G., Ineshin, E.M., Arzhannikova, A.V., Snopkov, S.V., 2010. The paleogeographic situation of human habitation in the river valleys in the Oka Plateau (East Sayan Ridge, Sentsa River valley). *Proceedings of the Laboratory of Ancient Technologies* 8, 291–302 (in Russian).

Arzhannikova, A., Arzhannikov, S., Jolivet, M., Vassallo, R., Chauvet, A., 2011. Pliocene to quaternary deformation in south east Sayan (Siberia): initiation of the tertiary compressive phase in the southern termination of the Baikal Rift System. *Journal of Asian Earth Sciences* 40, 581–594. <http://dx.doi.org/10.1016/j.jseas.2010.10.11>.

Balco, G., 2011. Contributions and unrealized potential contributions of cosmogenic nuclide exposure dating to glacier chronology, 1990–2010. *Quaternary Science Reviews* 30, 3–27.

Balco, G., Stone, J., Lifton, N., Dunai, T., 2008. A simple, internally consistent, and easily accessible means of calculating surface exposure ages and erosion rates from Be-10 and Al-26 measurements. *Quaternary Geochronology* 3, 174–195.

Benn, D.I., Lehmkühl, F., 2000. Mass balance and equilibrium-line altitudes in glaciers in high mountain environments. *Quaternary International* 65/66, 15–29.

Bennett, M.R., 2001. The morphology, structural evolution and significance of push moraines. *Earth-Science Reviews* 53, 197–236.

Bezrukova, E.V., Tarasov, P.E., Solovieva, N., Krivonogov, S.K., Riedel, F., 2010. Last glacial–interglacial vegetation and environmental dynamics in southern Siberia: chronology, forcing and feedbacks. *Palaeogeography, Palaeoclimatology, Palaeoecology* 296, 185–198.

Braucher, R., Brown, E.T., Bourlés, D.L., Colin, F., 2003. In situ produced  $^{10}\text{Be}$  measurements at great depths: implications for production rates by fast muons. *Earth and Planetary Science Letters* 211, 251–258.

Brown, E.T., Edmond, J.M., Raisbeck, G.M., Yiou, F., Kurz, M.D., Brook, E.J., 1991. Examination of surface exposure ages of Antarctic moraines using in situ produced Be-10 and Al-26. *Geochimica et Cosmochimica Acta* 55, 2269–2283.

Chersky, I.D., 1881. On the traces of an ancient glaciation in east Siberia (a system of the Lena river, lake Baikal, and the Irkut, Kitoi and Belaya rivers). *Proceedings of the East-Siberian Division of the Russian Geographical Society* 4/5, 2–7 (in Russian).

Chmieleff, J., von Blanckenburg, F., Kossert, K., Jakob, J., 2010. Determination of the  $^{10}\text{Be}$  half-life by multicollector ICP-MS and liquid scintillation counting. *Nuclear Instruments and Methods in Physics Research Section B* 268, 192–199.

De Henning-Michaelis, E.V., 1898. In north Mongolia: an expedition to the Munkusardyk and Kosogol in 1897. *Proceedings of the East-Siberian Division of the Russian Geographical Society* 29 (3) (in Russian).

Geological Map 1: 200 000, East Sayan Series, Sheet N-47-XXXIV, 1971. VSEGEI, Moscow.

Gillespie, A.R., Burke, R.M., Komatsu, G., Bayasgalan, A., 2008. Late Pleistocene glaciers in Darhad basin, northern Mongolia. *Quaternary Research* 69, 169–187.

Grosswald, M.G., 1965. *Geomorphological Development of the Sayan–Tuva Upland*. Nauka, Moscow, 166 p. (in Russian).

Grosswald, M.G., 1987. The late-glacial of the Sayany-Tuva highland: morphology, and the rate of filling of ice-dammed lakes. In: Kotikov, V.M., Grosswald, M.G. (Eds.), *Interaction of the Glaciation with the Atmosphere and the Ocean*. Academy of Sciences of the USSR, Nauka Press, Moscow, pp. 152–170 (in Russian).

Grosswald, M.G., Stenkevich, E.N., Uflyand, A.K., 1959. New Data on the Basalts of the Kamsara-Biikhem River Basin, Northeast Tuva. In: *Materials on Regional Geology*, vol. 5. Gosgeoltechizdat, Moscow (in Russian).

Ivanov, A.V., Arzhannikov, S.G., Demonterova, E.I., Arzhannikova, A.V., Orlova, L.A., 2011. Jom-Bolok Holocene volcanic field in the East Sayan Mts., Siberia, Russia: structure, style of eruptions, magma compositions and the first radiocarbon dating results. *Bulletin of Volcanology* 73, 1279–1294. <http://dx.doi.org/10.1007/s00445-011-0485-9>.

Jolivet, M., Arzhannikov, S., Arzhannikova, A., Chauvet, A., Vassallo, R., Braucher, R., 2011. Geomorphic Mesozoic and Cenozoic evolution in the Oka-Jombolok region (East Sayan ranges, Siberia). *Journal of Asian Earth Sciences*. <http://dx.doi.org/10.1016/j.jaes.2011.09.017>.

Komatsu, G., Arzhannikov, S.G., Arzhannikova, A.V., Ershov, K., 2007. Geomorphology of subglacial volcanoes in the Azas plateau, the Tuva Republic, Russia. *Geomorphology* 88, 312–328.

Komatsu, G., Arzhannikov, S.G., Gillespie, A.R., Burke, R.M., Miyamoto, H., Baker, V.R., 2009. Quaternary paleolake formation and cataclysmic flooding along the upper Yenisei River. *Geomorphology* 104, 143–164.

Korschinek, G., Bergmaier, A., Faestermann, T., Gerstmann, U.C., Knie, K., Rugel, G., Wallner, A., Dillmann, I., Dollinger, G., Lierse von Gostomski, ch., Kossert, K., Maitia, M., Poutivtsev, M., Remmert, A., 2010. A new value for the half-life of  $^{10}\text{Be}$  by heavy-ion elastic recoil detection and liquid scintillation counting. *Nuclear Instruments and Methods in Physics Research Section B* 268, 187–191.

Krivonogov, S.K., 2010. Late Pleistocene to Holocene Sedimentation in the Basins of the Baikal Rift Zone. Summary of the Thesis for the Degree of Doctor of Geology and Mineralogy, Irkutsk, p. 32 (in Russian).

Krivonogov, S.K., Sheinkman, V.S., Mistryukov, A.A., 2005. Ice damming of the Darhad paleolake (Northern Mongolia) during the late Pleistocene. *Quaternary International* 136, 83–94.

Kropotkin, P.A., 1867. A trip to the Oka post. *Proceedings of the Siberian Division of the Russian Geographical Society* 9/10, 1–94 (in Russian).



- Leonard, K.C., Fountain, A.G., 2003. Map-based methods for estimating glacier equilibrium-line altitudes. *Journal of Glaciology* 49 (166), 329–336.
- Matsera, A.V., 1993. Relief-forming role of glaciations in the eastern Sayan. *Geomorphology* 3, 84–92.
- Meierding, T.C., 1982. Late Pleistocene glacial equilibrium-line altitudes in the Colorado front range: a comparison of methods. *Quaternary Research* 18, 289–310.
- Merchel, S., Herpers, U., 1999. An update on radiochemical separation techniques for the determination of long-lived radionuclides via accelerator mass spectrometry. *Radiochimica Acta* 84, 215–219.
- Molchanov, I.A., 1934. East Sayan. In: *Outlines of geology of Siberia*, vol. 5. Izd-vo Akad. Nauk SSSR, p. 81 (in Russian).
- Nemchinov, V.G., Budaev, R.T., Rezanov, I.N., 1999. Pleistocene glaciations of the eastern Sayan Mountains. *Antropozoikum* 23, 11–15.
- Nesje, A., Dahl, S.O., 2000. *Glaciers and Environmental Change*. Oxford University Press, New York, New York, p 203.
- Obruchev, S.V., 1953. Eastern part of the Sayan-Tuva upland in the quaternary. *Proceedings of the All-Union Geographical Society* 85 (5), 533–546 (in Russian).
- Olyunin, V.N., 1965. Neotectonics and Glaciation of East Sayan. Nauka, Moscow, p 128. (in Russian).
- Peretolchin, S.P., 1908. Glaciers of the Munku-Sardyk ridge. *Proceedings of the Tomsk Technological Institute* 9 (1), 89 (in Russian).
- Putkonen, J., O'Neal, M., 2006. Degradation of unconsolidated quaternary landforms in the western North America. *Geomorphology* 75, 408–419.
- Rasskazov, S.V., Logatchev, N.A., Brandt, I.S., Brandt, S.B., Ivanov, A.V., 2000. *Geochronology and Geodynamics of the Late Cenozoic*. Nauka, Novosibirsk, p 288. (in Russian).
- Ravskii, E.I., Aleksandrova, L.P., Vangengeim, E.A., Gerbova, V.G., Golubeva, L.V., 1964. *Anthropogenic Deposits in the Southern East Siberia*. Nauka, Moscow, p 280. (in Russian).
- Romanovskii, N.N., 1993. *Fundamentals of Cryogenic Lithosphere*. University of Moscow Press, Moscow, p 336. (in Russian).
- Stone, J.O., 2000. Air pressure and cosmogenic isotope production. *Journal of Geophysical Research* 105, 23753–23759.
- Sugorakova, A.M., Yarmolyuk, V.V., Lebedev, V.I., 2003. Cenozoic volcanism of Tuva. *Tuva Institute of Integrated Resource Development SB RAS, Kyzyl*, p 92. (in Russian).
- Ufimtsev, G.F., Perevalov, A.V., Rezanova, V.P., Kulagina, N.V., Mashuk, I.M., Shetnikov, A.A., Rezanov, I.N., Shibanova, I.V., 2003. Radiothermoluminescence dating of quaternary sediments of the Tunka rift. *Russian Geology and Geophysics* 44 (3), 224–229.
- Voieikov, A.I., 1881. Climatological conditions of glacial phenomena: past and present. *Proceedings of the Mineralogical Society* 2, 16 (in Russian).
- Ward, G.K., Wilson, S.R., 1978. Procedures for comparing and combining radiocarbon age determinations: a critique. *Archaeometry* 20, 19–31.
- Yarmolyuk, V.V., Lebedev, V.I., Sugorakova, A.M., Bragin, V.Y., Litasov, Y.D., Prudnikov, S.T., Arakelyants, M.M., Lebedev, V.A., Ivanov, V.G., Kozlovskii, A.M., 2001. The Eastern Tuva region of neovolcanism in Central Asia: stages, products and types of volcanic activity. *Volcanology and Seismology* 3, 3–32 (in Russian).